CELL BIOLOGY

Lactate induces vascular permeability via disruption of VE-cadherin in endothelial cells during sepsis

Kun Yang[1,2]†, Min Fan[1,2]†, Xiaohui Wang[1,2], Jingjing Xu[1]‡, Yana Wang[1], P. Spencer Gill[1], Tuanzhu Ha[1,2], Li Liu[3], Jennifer V. Hall[1,2], David L. Williams[1,2], Chuanfu Li[1,2]*

Circulating lactate levels are a critical biomarker for sepsis and are positively correlated with sepsis-associated mortality. We investigated whether lactate plays a biological role in causing endothelial barrier dysfunction in sepsis. We showed that lactate causes vascular permeability and worsens organ dysfunction in CLP sepsis. Mechanistically, lactate induces ERK-dependent activation of calpain1/2 for VE-cadherin proteolytic cleavage, leading to the enhanced endocytosis of VE-cadherin in endothelial cells. In addition, we found that ERK2 interacts with VE-cadherin and stabilizes VE-cadherin complex in resting endothelial cells. Lactate-induced ERK2 phosphorylation promotes ERK2 disassociation from VE-cadherin. In vivo suppression of lactate production or genetic depletion of lactate receptor GPR81 mitigates vascular permeability and multiple organ injury and improves survival outcome in polymicrobial sepsis. Our study reveals that metabolic cross-talk between glycolysis-derived lactate and the endothelium plays a critical role in the pathophysiology of sepsis.

INTRODUCTION

Sepsis is a dysregulated immune response to infection that leads to multiple organ dysfunction and mortality (*1*). Disruption of endothelial cell (EC) barrier junctions plays a major role in multiple organ injury and mortality in sepsis (*2*, *3*). Substantial clinical evidence has shown that progressive tissue and body cavity edema typically develops in septic patients, suggesting widespread increases in vascular permeability (*4*, *5*). In addition, fluid resuscitation as a medical intervention could result in fluid overload with subsequent multiple organ failure and worsened outcomes of patients with sepsis (*6*). Therefore, therapies targeted at improving vascular homeostasis could provide an alternative approach for treating sepsis.

The EC monolayer, which lines all blood vessels, provides a critical barrier between the blood and tissues and regulates the movement of nutrients, fluid, and cells into the interstitial space (*7*). The integrity of this barrier is maintained by cell-cell adhesin molecules localized at junctions between ECs, including vascular endothelial cadherin (VE-cadherin) and tight junctions (claudin/occluding) (*2*). Disruption of VE-cadherin is sufficient to induce the disassembly of the blood vessel walls and increase the vascular permeability, leading to tissue edema (*8*). During sepsis, multiple cell-derived mediators, such as proinflammatory cytokines and damage-associated molecular patterns, impair the vascular barrier by inducing VE-cadherin endocytosis and degradation (*9*, *10*). However, less is known about the role of metabolic changes in regulating vascular integrity during sepsis.

Lactate, a major by-product of aerobic glycolysis, is known to accumulate in septic patients because of increased production (caused by hypoxia conditions and mitochondrial dysfunction) and decreased clearance (caused by kidney and liver injuries) (*11*). Therefore, high levels of serum lactate have been recognized as a critical biomarker for sepsis prognosis (*1*). According to the Sepsis-3 guidelines, persistent serum lactate levels over 2 mM, despite adequate fluid resuscitation, should be included as a new criterion when clinically defining septic shock (*1*). In addition, clinical observations indicate that persistently increased serum lactate positively correlates with organ dysfunction and mortality in sepsis (*12*). Of note, emerging evidence suggests that lactate is not only a biomarker but also a potent signaling molecule that regulates immune responses during sepsis (*13*, *14*). However, it remains unknown whether lactate can regulate EC barrier function and contribute to organ dysfunction in sepsis.

Here, we report a previously unidentified role of lactate in mediating vascular permeability during sepsis. We have demonstrated that lactate increases vascular permeability by disorganizing the VE-cadherin complex on the surface of ECs, resulting in multiple organ dysfunction in sepsis. The mechanisms involve lactate-induced phosphorylation of extracellular signal–regulated kinase 1/2 (ERK1/2) via G protein–coupled receptor 81 (GPR81) signaling. ERK1/2 phosphorylation promotes the activation of calpain1/2 for VE-cadherin proteolytic cleavage, followed by caveolin1/clathrin1-mediated endocytosis of VE-cadherin. In addition, we found that ERK2 interacts with VE-cadherin to maintain VE-cadherin stability in ECs. Phosphorylation of ERK2 induces the disassociation of ERK2 from VE-cadherin, which may sensitize lactate-induced VE-cadherin disruption and endocytosis. GPR81 inhibition attenuated lactate-induced vascular permeability and improved survival outcome in murine sepsis. Our study suggests that lactate generated from aerobic glycolytic metabolism plays an important biological role in mediating EC permeability by disruption of VE-cadherin–mediated adherens junction proteins on ECs.

RESULTS

Lactate promotes vascular permeability in polymicrobial sepsis

Clinical data show that serum lactate levels are positively correlated with sepsis-induced organ dysfunction and mortality (*15*, *16*). We

[1]Department of Surgery, James H. Quillen College of Medicine, East Tennessee State University, Johnson City, TN 37614, USA. [2]Center of Excellence in Inflammation, Infectious Disease, and Immunity, East Tennessee State University, Johnson City, TN 37614, USA. [3]Department of Geriatrics, The First Affiliated Hospital of Nanjing Medical University, Nanjing, Jiangsu 210029, China.
*Corresponding author. Email: li@mail.etsu.edu
†These authors contributed equally to this work.
‡Present address: Department of ICU, Harbin Medical University, Harbin, Heilongjiang 150081, China.

have previously reported that inhibition of glycolysis by hexokinase inhibitor 2-deoxyglucose (2-DG) attenuated sepsis-induced damage to heart, liver, and kidney, which is accompanied by suppressed lactate production (*17*). To better understand whether lactate could contribute to organ dysfunction during sepsis, we administered lactate (0.5 g/kg body weight) (*18*) to mice by intraperitoneal injection 6 hours after induction of cecal ligation and puncture (CLP) sepsis and examined cardiac function by echocardiography. As shown in Fig. 1 (A to C), sepsis significantly increased serum lactate levels (Fig. 1A) and decreased fractional shortening (FS, Fig. 1B) and ejection fraction (EF, Fig. 1C) by 26.9 and 20.6%, respectively, compared with sham controls. Elevation of serum lactate levels by lactate supplementation further worsened cardiac function in sepsis mice (Fig. 1, A to C). The FS% and EF% values were markedly decreased by 12.5 and 15.7% compared with vehicle-treated CLP septic mice (Fig. 1, B and C). In addition, CLP sepsis markedly induced kidney and liver injuries as evidenced by increased serum levels of creatinine (Fig. 1D) and aspartate aminotransferase (AST) (Fig. 1E). Lactate administration further increased serum levels of creatinine (Fig. 1D) and AST (Fig. 1E) in septic mice, suggesting that elevated lactate levels exaggerated liver and kidney injury during polymicrobial sepsis. Notably, liver injury is associated with impaired bacterial clearance in sepsis (*19*). We found that CLP mice with lactate supplementation, which induced worsened liver function, had higher levels of aerobic and anaerobic bacterial in the blood than in CLP mice treated with phosphate-buffered saline (PBS) (fig. S1). We have previously shown that suppression of lactate production by 2-DG improved survival outcome of CLP septic mice (*17*). As expected, lactate administration decreased survival rate of septic mice by 51.5% compared with vehicle-treated CLP septic mice (Fig. 1F).

Substantial evidence has shown that EC barrier damage contributes to sepsis-induced multiple organ dysfunction and mortality (*5*, *20*). To investigate whether sepsis-induced elevation of serum lactate levels contributes to vascular barrier dysfunction, we examined EC permeability by measuring Evans Blue dye (EBD) penetration into tissues (kidney and liver) as described previously (*21*). We observed

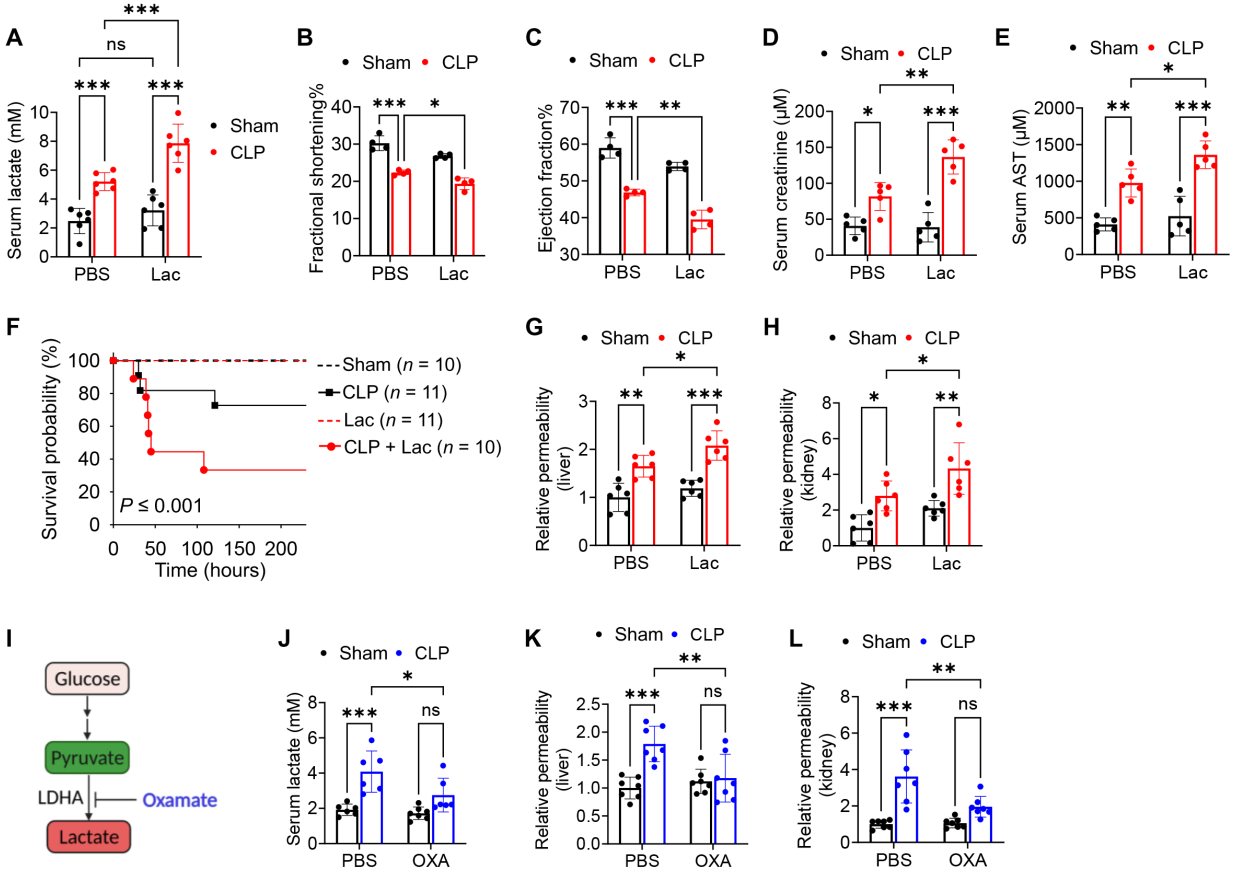

Fig. 1. Elevated lactate levels increase vascular permeability in polymicrobial sepsis. Lactate (0.5 g/kg body weight) was administrated through intraperitoneal injection 6 hours after CLP or sham surgery. (**A**) Serum lactate levels were assessed by a commercially available kit 24 hours after CLP/sham surgery ($n = 6$). (**B** and **C**) Left ventricular fraction shortening (FS) (B) and ejection fraction (EF) (C) were measured 24 hours after CLP/sham surgery ($n = 4$). (**D** and **E**) Serum levels of creatinine (D) and aspartate aminotransferase (AST) (E) were assessed by commercially available ELISA kits ($n = 5$). (**F**) Survival rates among sham, CLP, Lac, and CLP + Lac mice were compared by Kaplan-Meier test. (**G**) Relative levels of liver Evans Blue Dye (EBD) absorbance at 610 nm in sham and CLP mice with or without lactate administration ($n = 6$). (**H**) Relative levels of kidney EBD absorbance at 610 nm in sham and CLP mice with or without lactate administration ($n = 6$). (**I** and **J**) Sodium oxamate, an LDHA inhibitor, was administrated 3 hours before sham or CLP surgery to suppress lactate production (I). Serum lactate levels (**J**) were measured 24 hours following surgery ($n = 6$). (**K**) Relative levels of liver EBD absorbance at 610 nm in sham and CLP mice with or without oxamate administration ($n = 6$). (**L**) Relative levels of kidney EBD absorbance at 610 nm in sham and CLP mice with or without oxamate administration ($n = 6$). Values are means ± SD. Lac, lactate. OXA, sodium oxamate. LDHA, lactate dehydrogenase A. CLP, cecal ligation and puncture. Two-way ANOVA with Tukey's test. $^*P < 0.05$; $^{**}P < 0.01$; $^{***}P < 0.001$. ns, no significant difference.

that CLP sepsis significantly caused vascular permeability as evidenced by the increased penetration of EBD in liver (Fig. 1G) and kidney (Fig. 1H). Notably, administration of supplemental lactate further increased sepsis-induced vascular permeability in liver (Fig. 1G) and kidney (Fig. 1H). Similarly, we observed that lactate increased vascular permeability of liver, kidney, and lung in a sterile sepsis model induced by lipopolysaccharide (LPS) (fig. S2, A to C). To confirm the role of lactate in sepsis-induced vascular permeability, we treated mice with sodium oxamate (0.75 g/kg body weight), an inhibitor of lactate dehydrogenase A, to suppress lactate production (Fig. 1I) before induction of CLP sepsis and assessed vascular permeability in kidney and liver. Consistent with our previous report (*17*), suppression of lactate production by oxamate (Fig. 1J) significantly attenuated CLP-induced vascular permeability in both liver (Fig. 1K) and kidney (Fig. 1L), accompanied by decreased serum levels of AST (fig. S3A) and creatinine (fig. S3B). Together, these data suggest that lactate, generated from sepsis-increased aerobic metabolism, plays an important biological role in promoting vascular permeability and organ injuries during sepsis.

Lactate disrupts VE-cadherin junction on ECs

VE-cadherin is an important adherens junction protein that plays a crucial role in the maintenance of EC junction and vascular integrity (*22*). Disruption of the VE-cadherin complex impairs endothelium barrier function (*22*). Next, we sought to assess whether lactate-promoted endothelium barrier dysfunction is mediated by disrupting VE-cadherin on ECs. To achieve this, we induced polymicrobial sepsis in the mice with EC-specific expression of green fluorescent protein (GFP) [Tg(TIE2GFP)287Sato] (*23*) with and without supplemental lactate. Twenty-four hours after induction of polymicrobial sepsis, we isolated the ECs from heart, liver, and kidney tissues and analyzed VE-cadherin by flow cytometry using anti–VE-cadherin (CD144) antibody. As shown in Fig. 2A, sepsis decreased VE-cadherin (CD144) levels on the membrane of ECs that were isolated from heart, liver, and kidney tissues by 13.1, 73.6, and 30.3%, respectively, compared with sham controls. Administration of lactate further decreased VE-cadherin expression on ECs of heart, liver, and kidney by 16.5, 47.9, and 10.4%, respectively, compared with ECs isolated from vehicle-treated sepsis mice (Fig. 2A). Immunofluorescent staining with anti–VE-cadherin antibody showed that polymicrobial sepsis decreased VE-cadherin levels on ECs in the lung tissues, which was further decreased by lactate supplementation (Fig. 2B). Consistently, Western blot analysis showed that the expression of VE-cadherin was decreased in the heart (Fig. 2C) and lung (Fig. 2D) lysates following sepsis, which was further decreased by lactate administration. Conversely, inhibition of lactate production by oxamate attenuated CLP sepsis–induced decrease of VE-cadherin levels in the heart (Fig. 2E) and lung (Fig. 2F) lysates. These data suggest that lactate could contribute to vascular permeability by disrupting VE-cadherin on ECs during sepsis.

We then treated human umbilical vein ECs (HUVECs) with an increased lactate concentration and examined VE-cadherin protein levels. As shown in fig. S4A, lactate at 10 mM significantly reduced VE-cadherin protein levels in ECs. Lactate administration increased EC permeability as evidenced by increased penetration of fluorescein isothiocyanate (FITC)–conjugated dextran. Treatment of HUVECs with acidic condition that was equal to lactate condition did not promote EC permeability (fig. S4B), suggesting that lactate, but not acidic condition, could cause EC barrier dysfunction. Immunofluorescent staining with anti–VE-cadherin antibody showed that lactate disengaged VE-cadherin on the cell surface in both HUVECs (fig. S4C) and human cardiac microvascular ECs (HCMECs) (fig. S4D). In agreement, lactate treatment markedly reduced the levels of VE-cadherin on the membrane fraction of ECs (fig. S4E). In addition, a Matrigel-based tube formation assay also showed that lactate administration disrupted tube formation of HUVECs compared with vehicle-treated controls (fig. S4F). Notably, flow cytometry analysis showed that lactate treatment did not significantly induce EC death and apoptosis (fig. S4G). In addition, lactate treatment did not significantly alter VE-cadherin transcription (fig. S4H) or induced VE-cadherin phosphorylation in ECs (fig. S4I). It is reported that VE growth factor (VEGF) induces VE-cadherin phosphorylation, contributing to endocytosis of VE-cadherin and increased vascular permeability (*22*). We examined serum VEGF levels of CLP sepsis mice and found that CLP induced elevation of serum VEGF (fig. S4J). However, administration of lactate or suppression of lactate production by oxamate had no significant effects on CLP-increased VEGF levels (fig. S4J). Collectively, these data suggest that lactate induces VE-cadherin disruption, resulting in dysfunction of EC barrier.

Lactate disrupts the colocalization of VE-cadherin with ERK2 at the plasma membrane of ECs

ERK1/2 has been reported to localize on cellular compartments, such as Golgi apparatus (*24*), mitochondrial membrane (*25*), and plasma membrane (*26*). In addition, a recent study indicates that ERK is required to maintain endothelium integrity (*27*). However, it is unclear whether ERK can stabilize endothelial adherens junction via interacting with the VE-cadherin complex. To address this question, we first evaluated the localization of ERK1/2 by immunofluorescence staining. Compared with sparse culture of ECs, ERK1/2 (green color) colocalized with VE-cadherin (red color) on the surface of confluent ECs upon the formation of adherens junction (Fig. 3A). Consistently, Western blot analysis using membrane lysate of ECs showed the presence of ERK1/2 protein (Fig. 3B). We then examined the protein levels and localization of ERK in lactate-treated ECs by immunoblotting and immunofluorescence staining. As shown in Fig. 3B, lactate (10 mM) treatment strongly decreased membrane ERK levels in ECs. Immunofluorescent staining using anti–VE-cadherin and anti-ERK1/2 antibodies further showed that lactate induced disassociation of ERK1/2 (green color) from VE-cadherin (red color) at the membrane plasma, which is accompanied by VE-cadherin disruption in ECs (Fig. 3C). To confirm the interaction between ERK and VE-cadherin, we performed immunoprecipitation assays and observed that lactate treatment reduced VE-cadherin levels in the ERK1/2 immunoprecipitants (Fig. 3D). It is reported that ERK1 and ERK2 are expressed at different levels and have distinct functions in cellular processes (*28*–*30*). We observed that ERK2 has significantly higher expression levels than ERK1 in the membrane fraction of ECs (Fig. 3E). Immunoprecipitation with anti-ERK1 and anti-ERK2 antibodies followed by immunoblotting with anti–VE-cadherin showed that ERK2, but not ERK1, interacts with VE-cadherin in ECs (Fig. 3, F and G). Lactate treatment induced disassociation of ERK2 from VE-cadherin in ECs (Fig. 3F). These data suggest that ERK2 and VE-cadherin are colocalized on the membrane of ECs. Lactate treatment can induce the disassociation between ERK2 and VE-cadherin in ECs.

To investigate whether lactate could promote ERK phosphorylation, resulting in the dissociation of ERK2 from VE-cadherin on the

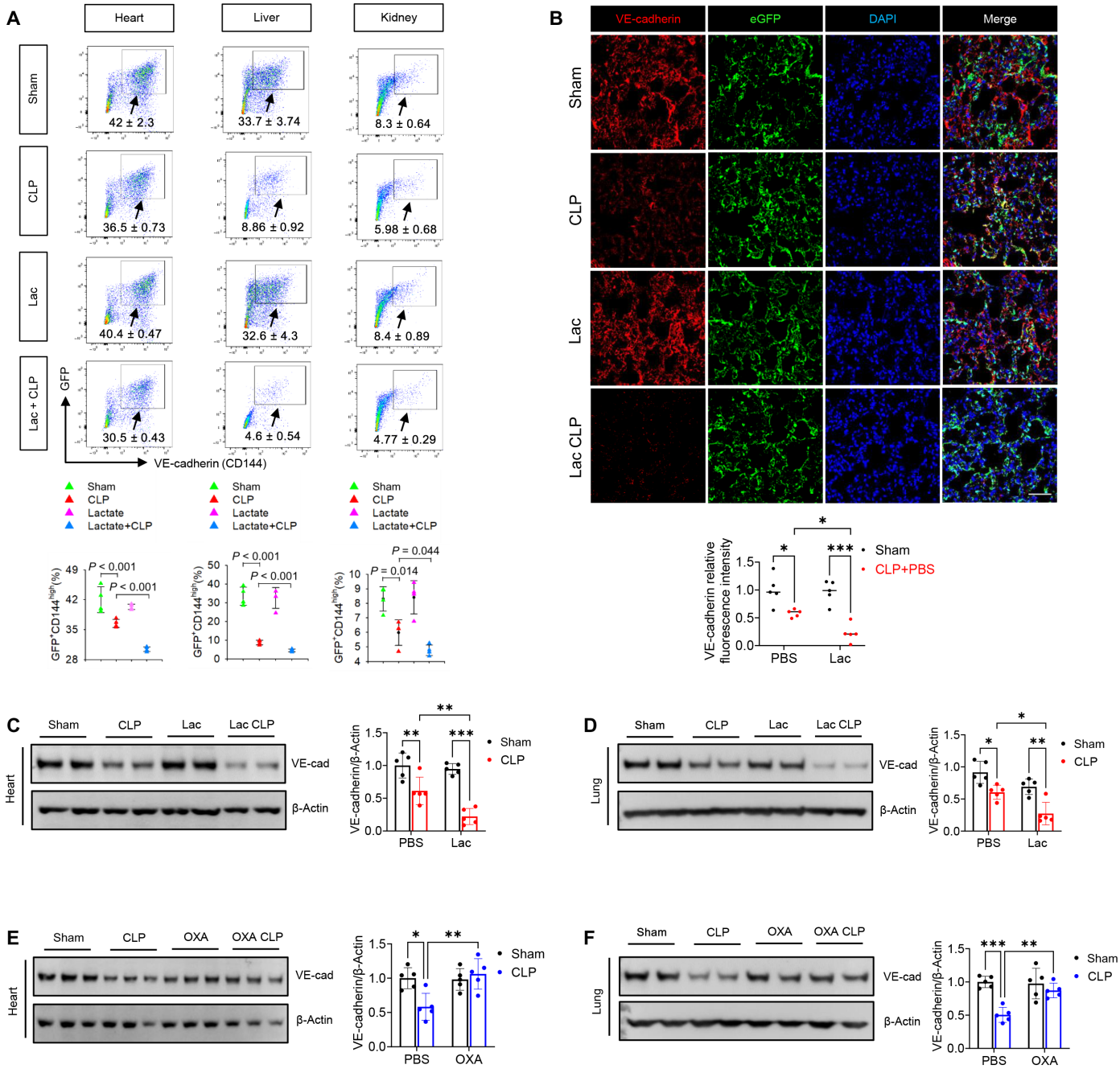

Fig. 2. Lactate decreases VE-cadherin levels following polymicrobial sepsis. (**A**) Representative flow density plot and quantitative analysis for VE-cadherin (CD144)–positive EC frequency in the tissues of Tie2-GFP reporter mice ($n = 4$). (**B**) Representative immunofluorescent staining images of GFP-labeled EC (green), VE-cadherin (red), and nuclei (DAPI, blue) in the lung tissues of Tie2-GFP reporter mice. Scale bar, 100 μm. (**C**) Western blot detection of VE-cadherin protein expression in whole heart lysates of sham, CLP, Lac, and Lac + CLP mice ($n = 5$). (**D**) Western blot detection of VE-cadherin protein expression in whole lung lysates of sham, CLP, Lac, and Lac + CLP mice ($n = 5$). (**E**) Western blot detection of VE-cadherin protein expression in whole heart lysates of sham, CLP, OXA, and OXA + CLP mice ($n = 5$). (**F**) Western blot detection of VE-cadherin protein expression in whole lung lysates of sham, CLP, OXA, and OXA + CLP mice ($n = 5$). VE-cad, VE-cadherin. Two-way ANOVA with Tukey's test. $^*P < 0.05$; $^{**}P < 0.01$; $^{***}P < 0.001$.

membrane of ECs, we first examined ERK1/2 phosphorylation in lactate-treated ECs. Lactate treatment markedly increased the levels of phosphorylated ERK1/2 by 82.4% compared with untreated control (Fig. 3H). We also performed immunostaining with anti–phosphorylated ERK1/2. In contrast to the ERK1/2, we observed that the phosphorylated ERK1/2 is exclusively localized in the cytoplasm of ECs (Fig. 3I). To confirm that ERK phosphorylation is an important step for lactate-induced disruption of VE-cadherin integrity on the membrane of ECs, we treated ECs with LY3214996 to suppress ERK1/2 phosphorylation before lactate stimulation. As shown

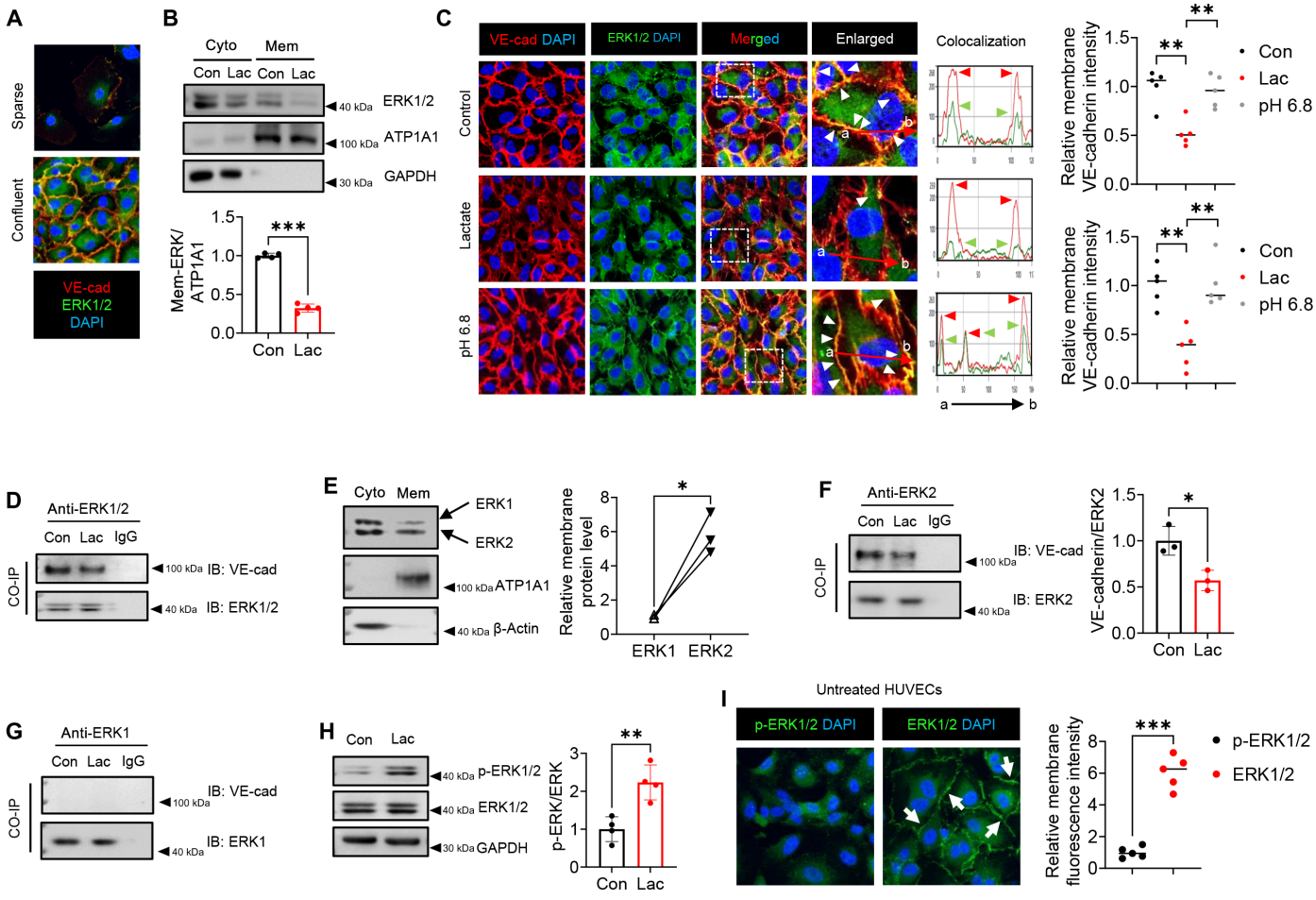

Fig. 3. Lactate promotes VE-cadherin disorganization by inducing ERK1/2 phosphorylation and decreasing junctional ERK2 expression. (**A**) Representative immunofluorescent staining images of VE-cadherin (red), ERK (green), and nuclei (DAPI, blue) in sparse and confluent HUVECs. (**B**) HUVECs were treated with lactate for 6 hours followed by Western blot analysis of the ERK protein levels in the membrane fraction ($n = 4$). (**C**) Representative immunofluorescent staining images of VE-cadherin (red), ERK (green), and nuclei (DAPI, blue) in HUVECs treated with lactate or acidic medium (pH 6.8) for 6 hours. Colocalization between ERK and VE-cadherin staining was analyzed by plotting fluorescence intensity profiles along red arrow lines using ZEN 3.1 (blue edition). White arrowheads indicate the colocalization of ERK with VE-cadherin at the plasma membrane in HUVECs ($n = 5$). (**D**) HUVECs were treated with lactate for 6 hours. Protein lysates (200 μg) were precipitated with anti-ERK1/2 antibody followed by immunoblotting with anti–VE-cadherin antibody. (**E**) Western blot analysis of ERK1/2 levels in cytosolic and membrane fractions of untreated HUVECs ($n = 3$). (**F** and **G**) HUVECs were treated with lactate for 6 hours. Protein lysates (200 μg) were precipitated with anti-ERK2 (F) and anti-ERK1 (G) antibodies followed by immunoblotting with anti–VE-cadherin antibody ($n = 3$). (**H**) Western blot analysis of p-ERK and ERK expressions in lactate-treated ECs ($n = 3$). (**I**) Representative immunofluorescent staining images of p-ERK and ERK in confluent HUVECs. White arrows indicate membrane ERK staining in HUVECs. Membrane levels of p-ERK1/2 and ERK1/2 fluorescence were analyzed by ZEN 3.1 (blue edition) ($n = 5$). mem, membrane fraction. Cyto, cytosol fraction. CO-IP, co-immunoprecipitation. Student's two-tailed unpaired *t* test (B, E, F, H, and I). One-way ANOVA with Tukey's test (C). $^*P < 0.05$; $^{**}P < 0.01$; $^{***}P < 0.001$.

in fig. S5 (A and B), inhibition of ERK1/2 phosphorylation by LY3214996 attenuated lactate-induced disassociation of ERK with VE-cadherin on the plasma membrane and abolished lactate-induced VE-cadherin disruption on ECs. We have observed that ERK2, instead of ERK1, interacts with VE-cadherin at the membrane of EC. To further dissect whether lactate-induced ERK2 phosphorylation and disassociation from VE-cadherin contribute to lactate-induced VE-cadherin disruption, we transfected HUVECs with either wild-type ERK2 (WT-ERK2) or mutant ERK2T183A/Y185F (MU-ERK2) plasmids (*31*). The MU-ERK2 cannot be phosphorylated or activated (fig. S6B), and both WT and MU-ERK2 plasmids were labeled with enhanced GFP (*31*). As shown in fig. S6A, upon transient transfection, WT-ERK2 and MU-ERK2 were distributed throughout the cell body, including the membrane (arrows). Immunoprecipitation with anti-GFP antibody followed by immunoblotting with anti–VE-cadherin showed that both WT-ERK2 and MU-ERK2 interact with VE-cadherin in ECs (fig. S6B). Notably, forced inactivation of ERK2 (MU-ERK2) attenuated lactate-induced ERK2 disassociation from VE-cadherin (fig. S6B) and maintained VE-cadherin integrity and expression in lactate-treated ECs (fig. S6, A and C). Together, these data suggest that the colocalization of ERK2 with VE-cadherin on the membrane of ECs is important for the stabilization of VE-cadherin–mediated adherens junction of ECs and that ERK2 phosphorylation could be responsible for lactate-induced VE-cadherin disruption by disassociation of VE-cadherin with ERK.

Lactate-induced ERK1/2 phosphorylation is mediated by cAMP/RAF1/MEK signaling

It is reported that lactate activates GPR81 and inhibits the formation of second messenger cyclic adenosine monophosphate (cAMP) via adenylyl cyclase (Fig. 4A) (*32*). cAMP inhibits ERK signaling in various cell types (*33*–*35*). To investigate whether lactate-induced ERK phosphorylation is mediated by suppression of cAMP formation, we treated ECs with cAMP-elevating agent, forskolin, before lactate stimulation. Forskolin directly activates adenylyl cyclase and raises cAMP levels (Fig. 4A) (*35*). As shown in Fig. 4 (B and C), forskolin attenuated lactate-induced VE-cadherin disruption and lactate-induced decreases in VE-cadherin levels in ECs. In addition, forskolin also attenuated lactate-induced ERK1/2 phosphorylation (Fig. 4D). Previous studies indicate that cAMP inhibits RAF1/mitogen-activated protein kinase kinase (MEK) signaling, which contributes to ERK inactivation (*36*, *37*). We observed that forskolin diminished lactate-induced RAF1/MEK/ERK activation (Fig. 4D). In addition, silencing of MEK1/2 by their specific small interfering RNAs (siRNAs) before lactate treatment suppressed lactate-induced ERK1/2 phosphorylation and VE-cadherin down-regulation in ECs (Fig. 4E), suggesting that lactate induced ERK phosphorylation, and VE-cadherin disruption is mediated, at least in part, by cAMP/RAF1/MEK signaling. The exchange protein directly activated by cAMP (EPAC) is a critical effector protein of cAMP (*38*). Several lines of evidence implicate that cAMP-mediated EPAC activation stabilizes VE-cadherin via regulating cytoskeleton dynamics in HUVECs (*39*, *40*). Of note, a recent study shows that administration of EPAC agonist reduced lactate-induced bone marrow vascular permeability (*21*). Consistent with this observation, we found that pretreatment of EPAC agonist maintained VE-cadherin integrity (Fig. 4F) and VE-cadherin protein levels (Fig. 4G) in lactate-stimulated ECs. However, EPAC agonist had no effects on lactate-induced activation of RAF1/MEK/ERK signaling (Fig. 4H). These data suggest that both suppression of cAMP/EPAC signaling and activation of RAF1/MEK/ERK signaling contribute to lactate-induced VE-cadherin disruption in ECs (Fig. 4A). This conclusion is supported by the observation that inhibition of MEK/ERK signaling synergizes the permeability-reducing effect of EPAC agonist (*41*).

Lactate increases calpain activity via ERK phosphorylation for VE-cadherin disruption

Activation of calpain, which is a Ca^{2+}-dependent intracellular cysteine protease, has been reported to mediate the proteolytic disorganization of VE-cadherin (*42*). Therefore, we examined whether lactate could induce calpain activation for VE-cadherin proteolytic cleavage on ECs. In vivo data show that polymicrobial sepsis increased the levels of calpain1 in heart (fig. S7A) and lung (fig. S7B) tissue lysates compared with sham control, which was further increased by administration of supplemental lactate in septic mice. Immunofluorescent staining of lung tissues with anti-calpain1, anti-calpain2, and anti-CD31 antibodies showed that polymicrobial sepsis increased levels of calpain1 (red color, Fig. 5A) and calpain2 (red color, Fig. 5B) in ECs, as compared with sham control. Notably, administration of supplemental lactate further increased levels of endothelial calpian1/2 in lung tissue (Fig. 5, A and B) of septic mice, when compared with vehicle-treated septic mice. To validate these observations, we performed in vitro experiments using ECs treated with or without lactate. As shown in Fig. 5C, lactate markedly increased calpain1/2 protein levels in ECs in a time-dependent manner. In addition, lactate treatment significantly up-regulated total calpain enzyme activity in ECs (Fig. 5D). These data suggest that lactate can increase calpain expression and enzyme activity in ECs during polymicrobial sepsis.

We then investigated the role of calpain in lactate-induced VE-cadherin disruption on ECs. As shown in Fig. 5E, lactate treatment disrupted VE-cadherin (red color) and increased levels of calpain1 (green color) in ECs. There is an interaction between calpain1 (green) and VE-cadherin (red) in the merged image (white arrow) in lactate-treated ECs (Fig. 5E). Immunoprecipitation assay shows that lactate increased calpain1 (Fig. 5F) and calpain2 (Fig. 5G) levels in the VE-cadherin immunoprecipitants. To assess whether calpain activation is required for the proteolytic cleavage of VE-cadherin in lactate-treated ECs, we silenced calpain1 and calpain2 with specific siRNAs and examined VE-cadherin levels in the ECs treated with and without lactate. As shown in fig. S8 (A and B), lactate treatment significantly decreased VE-cadherin levels. However, silencing of calpain1 (fig. S8A) or calpain2 (fig. S8B) markedly attenuated lactate-induced decreases in VE-cadherin in ECs. Similarly, treatment of ECs with calpeptin, a calpain inhibitor, also attenuated lactate-induced decreases in VE-cadherin (fig. S8C). These data indicate that lactate-induced activation of calpain can contribute to proteolytic cleavage of VE-cadherin in ECs.

Previous studies have demonstrated that ERK phosphorylation leads to calpain activation (*43*, *44*). We observed that lactate induced ERK phosphorylation in ECs (Fig. 3H). To dissect whether lactate-increased calpain expression and enzyme activity are mediated by ERK phosphorylation, we treated ECs with LY3214996 before lactate stimulation. Figure S5B shows that inhibition of ERK phosphorylation by LY3214996 markedly attenuated lactate-induced increases in calpain1/2 levels and lactate-induced decreases in VE-cadherin levels in ECs. Collectively, these data suggest that lactate can promote ERK-dependent activation of calpain1/2 in ECs. Consequently, activated calpain1/2 induces VE-cadherin proteolytic cleavage and degradation.

Lactate promotes clathrin1- and caveolin1-mediated endocytosis of VE-cadherin

Next, we sought to determine whether lactate-induced calpain-mediated proteolytic cleavage of VE-cadherin could result in VE-cadherin endocytosis, resulting in decreased VE-cadherin levels on the membrane of ECs. We first examined the levels of endocytosis mediators, such as clathrin1, caveolin1, rab11, and rab5 in the ECs treated with and without lactate (*45*). Our data show that the levels of clathrin1 and caveolin1, but not rab11 and rab5, were significantly increased in lactate-treated ECs in a time- and dose-dependent manner (fig. S9, A to C). We then focused on clatherin1- and caveolin1-mediated endocytosis of VE-cadherin. Immunofluorescence staining with anti–VE-cadherin, anti-clathrin1, and anti-caveolin1 antibodies shows that lactate induced VE-cadherin internalization into caveolin1 (fig. S9D) and clathrin1 (fig. S9E) endosomes in ECs, as evidenced by colocalization of VE-cadherin with clathrin1 or caveolin1. Enhanced VE-cadherin internalization was also accompanied by disrupted VE-cadherin complex on the cell surface of ECs (fig. S9, D and E). Consistently, immunoprecipitation with anti–VE-cadherin followed by immunoblotting with anti-caveolin1 also showed that lactate markedly increased caveolin1 levels in the VE-cadherin immunocomplex (fig. S9F). To further confirm the role of clatherin1- and caveolin1-mediated endocytosis of VE-cadherin in lactate-induced disruption of VE-cadherin on the surface of ECs, we treated

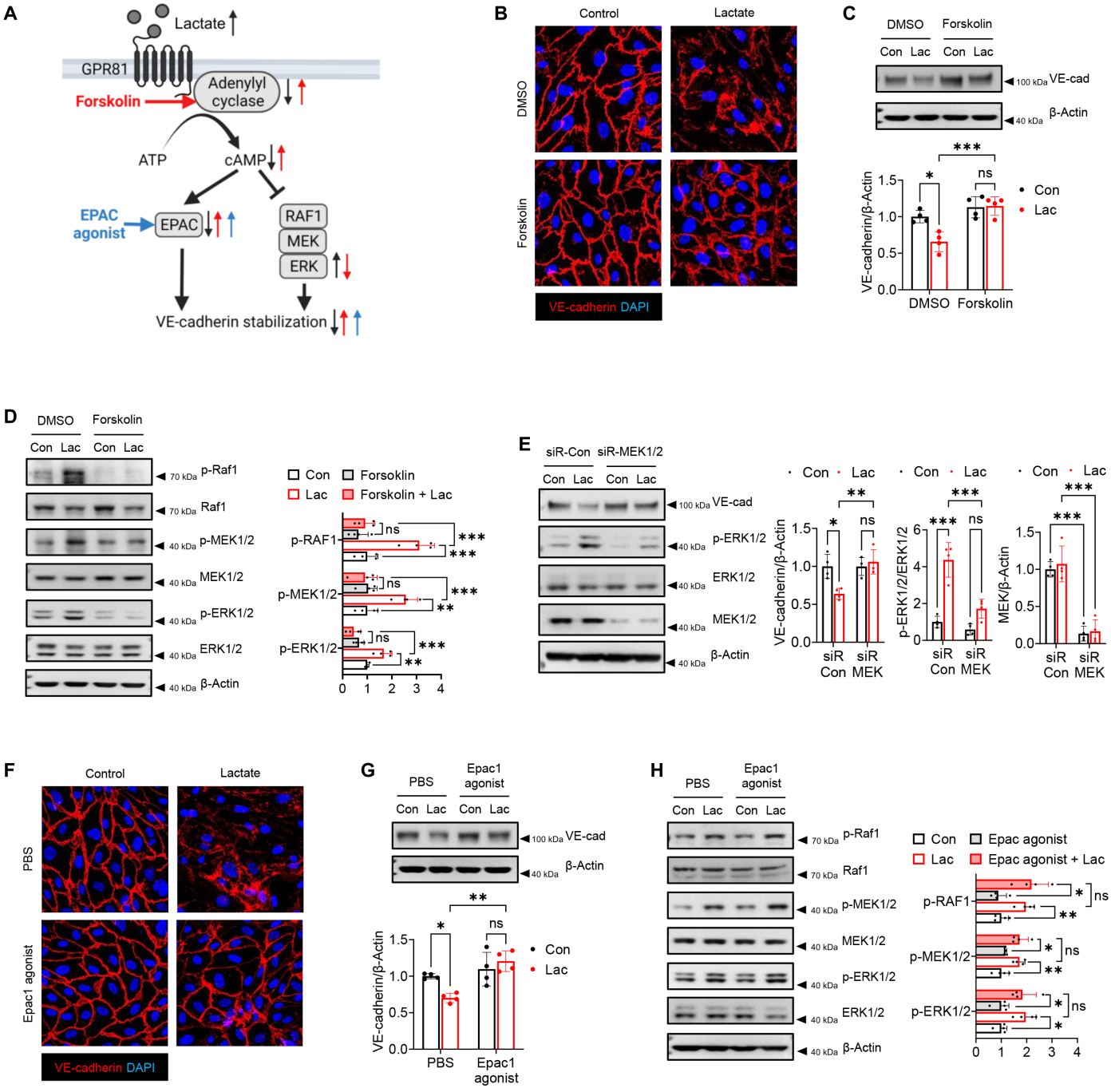

Fig. 4. Lactate-suppressed adenylyl cyclase activity contributes to VE-cadherin down-regulation by activation of RAF1/MEK/ERK signaling. (**A**) A scheme depicting lactate mode of action in regulating VE-cadherin stability via GPR81/cAMP signaling. (**B**) HUVECs were treated with adenylyl cyclase activator (forskolin, 10 μM) before lactate stimulation for 6 hours. Representative immunofluorescent staining images of VE-cadherin (red) and nuclei (DAPI, blue) in HUVECs. (**C**) Western blot analysis of VE-cadherin in HUVECs pretreated with forskolin followed by lactate stimulation for 6 hours ($n = 4$). (**D**) Western blot analysis of RAF1/MEK/ERK signaling in HUVECs pretreated with forskolin followed by lactate stimulation ($n = 4$). (**E**) HUVECs were transfected with siRNAs for MEK1/MEK2 and scramble control siRNA for 24 hours before lactate stimulation for 6 hours. Expression of VE-cadherin, p-ERK1/2, and MEK1/2 were assessed by Western blot ($n = 4$). (**F**) HUVECs were treated with EPAC agonist (8-CPT-2Me-cAMP, 100 μM) before lactate stimulation for 6 hours. Representative immunofluorescent staining images of VE-cadherin (red) and nuclei (DAPI, blue) in HUVECs. (**G**) Western blot analysis of VE-cadherin in HUVECs pretreated with EPAC agonist followed by lactate stimulation for 6 hours ($n = 4$). (**H**) Western blot analysis of RAF1/MEK/ERK signaling in HUVECs pretreated with forskolin followed by lactate stimulation ($n = 4$). EPAC, exchange protein directly activated by cAMP. Con, control. Two-way ANOVA with Tukey's test. $^*P < 0.05$; $^{**}P < 0.01$; $^{***}P < 0.001$.

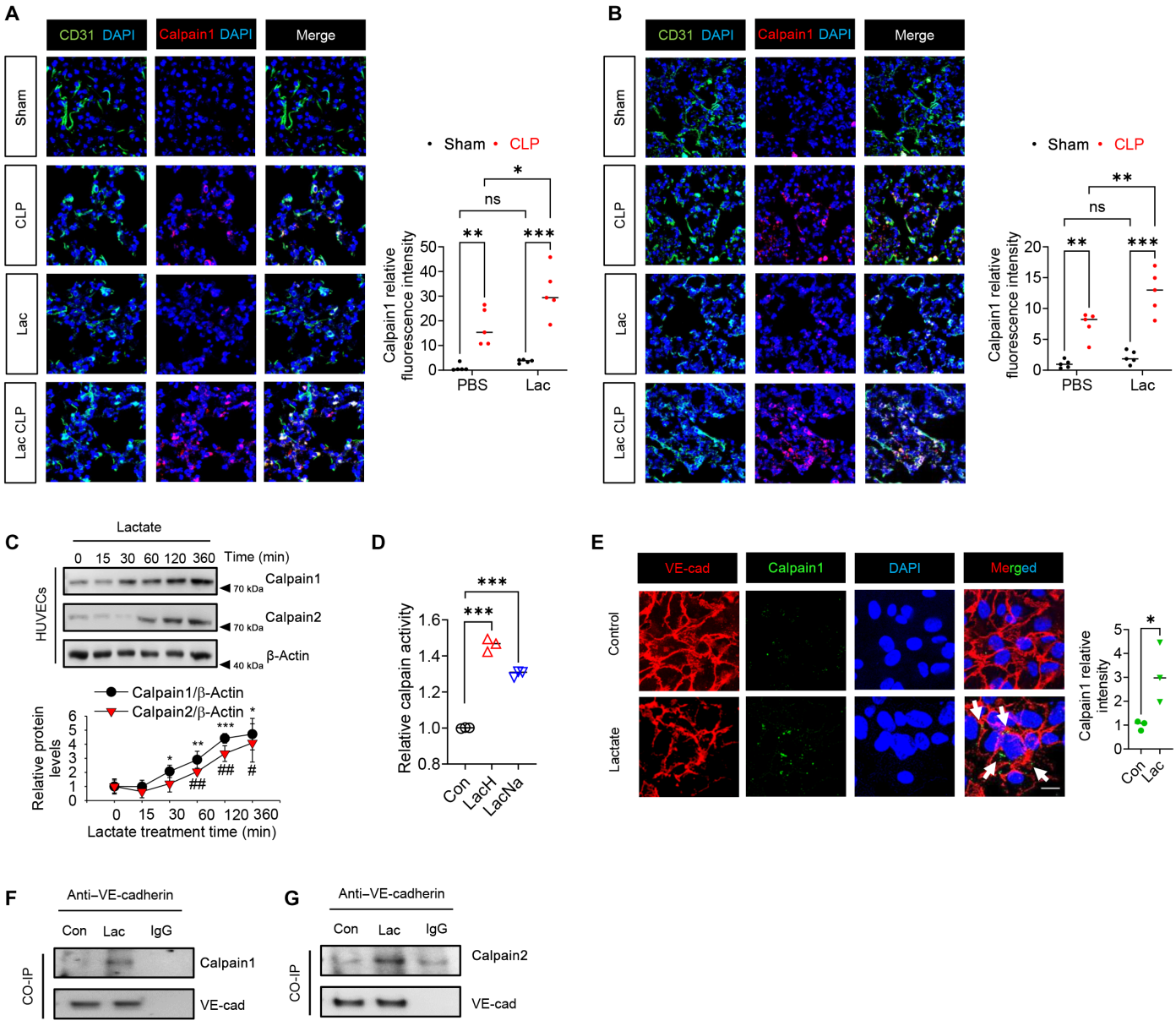

Fig. 5. Calpain activation is required for lactate-induced disruption of VE-cadherin in ECs. Lactate (0.5 g/kg body weight) was administrated through intraperitoneal injection 6 hours after CLP or sham surgery. (**A** and **B**) Representative immunofluorescent staining images of calpain1 (red, A) and calpain2 (red, B) in ECs of the lung tissues. ECs were stained with CD31 (green), and nuclei were stained with DAPI (blue) ($n = 5$). (**C**) Western blot analysis of calpain1 and calpain2 expressions following lactate treatment in ECs ($n = 3$). (**D**) Calpain enzyme activity in ECs treated with lactic acid or sodium lactate ($n = 3$). (**E**) Representative immunofluorescent staining images of VE-cadherin (red), calpain1 (green), and nuclei (DAPI, blue) in HUVECs treated with or without lactate ($n = 3$). Scale bar, 20 μm. (**F** and **G**) HUVECs were treated with lactate for 6 hours. Protein lysates (200 μg) were precipitated with anti–VE-cadherin antibody followed by immunoblotting with anti-calpain1 (F) or anti-calpain2 (G) antibodies. LacH, lactic acid. LacNa, sodium lactate. Two-way ANOVA with Tukey's test (A and B). One-way ANOVA with Tukey's test (C and D). Student's two-tailed unpaired *t* test (E). $^*P < 0.05$; $^{**}P < 0.01$; $^{***}P < 0.001$.

ECs with dynamin inhibitors to suppress the endocytosis before lactate treatment and examined VE-cadherin levels in HUVECs. Dynamin is a large guanosine triphosphate, which is necessary for clathrin1- and caveolin1-dependent endocytosis by assembling into polymers on the necks of budding membranes and facilitating the membrane fission (fig. S9G) (*45*). We found that suppression of endocytosis by dynamin inhibitor (Dynasore, DNSR) prevented lactate-induced decreases in the levels of VE-cadherin in ECs (fig. S9H). Together, our data suggest that disorganized VE-cadherin induced by lactate is susceptible to caveolin1-/clathrin1-dependent endocytosis.

Calpain1/2 inhibition abolished lactate-induced endocytosis of VE-cadherin in ECs

The above data show that lactate activates calpain1/2 for VE-cadherin proteolytic disorganization, leading to clathrin1-/caveolin1-dependent

endocytosis of VE-cadherin in ECs (fig. S9). To investigate whether inhibition of calpain1/2 could prevent clathrin1-/caveolin1-mediated endocytosis of VE-cadherin, we treated ECs with the calpain inhibitor, calpeptin, before lactate treatment and examined the association between VE-cadherin and caveolin1/clathrin1 by immunoprecipitation. Figure 6 (A and B) shows that lactate treatment increased caveolin1 and clathrin1 levels in VE-cadherin immunoprecipitants. However, calpain inhibition by calpeptin significantly attenuated lactate-induced increases in caveolin1 (Fig. 6A) and clathrin1 (Fig. 6B) levels in VE-cadherin immunoprecipitants. Similarly, lactate treatment increased VE-cadherin in both caveolin1 immunoprecipitants (Fig. 6C) and clathrin1 immunoprecipitants (Fig. 6D), which were attenuated by inhibition of calpain1/2 with calpeptin. In agreement with this, silencing of calpain1 or calpain2 by specific siRNAs strongly reduced VE-cadherin protein levels in caveolin1 (fig. S10A) and clathrin1 (fig. S10B) immunoprecipitants of lactate-treated ECs. We also performed immunofluorescent staining to examine the effect of calpain1/2 inhibition on the colocalization of VE-cadherin with clathrin1 or caveolin1 in ECs treated with or without lactate. Our data show that lactate treatment disrupted VE-cadherin on the plasma membrane of ECs and induced colocalization of VE-cadherin with caveolin1 (white arrows, Fig. 6E) or clathrin1 (white arrows, Fig. 6F). However, calpain inhibition by calpeptin prevented lactate-induced VE-cadherin disorganization and caveolin1-/clathrin1-mediated endocytosis (Fig. 6, E and F). As expected, silencing of calpain1/2 by their specific siRNAs showed consistent results (fig. S10, C and D). Collectively, these data suggest that lactate promoted calpain1/2-mediated proteolytic cleavage of VE-cadherin, which subsequently leads to caveolin1-/clathrin1-dependent endocytosis of VE-cadherin.

Lactate induces VE-cadherin disorganization via GPR81

GPR81 is a receptor for lactate (*18*, *32*, *46*). We investigated whether lactate-induced VE-cadherin disorganization and endocytosis are mediated via GPR81-dependent signaling. GPR81 was silenced in ECs by transfection with its specific siRNA before lactate treatment, and VE-cadherin levels were examined. Our data show that knockdown of GPR81 significantly attenuated lactate-induced decreases in VE-cadherin levels (Fig. 7A) and prevented lactate-induced disruption of VE-cadherin at the plasma membrane of ECs (Fig. 7B). The in vitro permeability assay showed that silencing of GPR81 prevented lactate-induced hyperpermeability of endothelium (Fig. 7C). Consistently, treatment of ECs with the GPR81 antagonist 3-hydroxybutyrate acid (3-OBA) also attenuated lactate-induced decreases in VE-cadherin (Fig. 7D) and lactate-induced endothelium hyperpermeability (Fig. 7E). In addition, GPR81 inhibition by 3-OBA attenuated lactate-induced ERK1/2 phosphorylation and lactate-increased calpain1/2 levels in ECs (Fig. 7F). Monocarboxylate transporter 1 (MCT1) is a lactate transporter involved in the influx

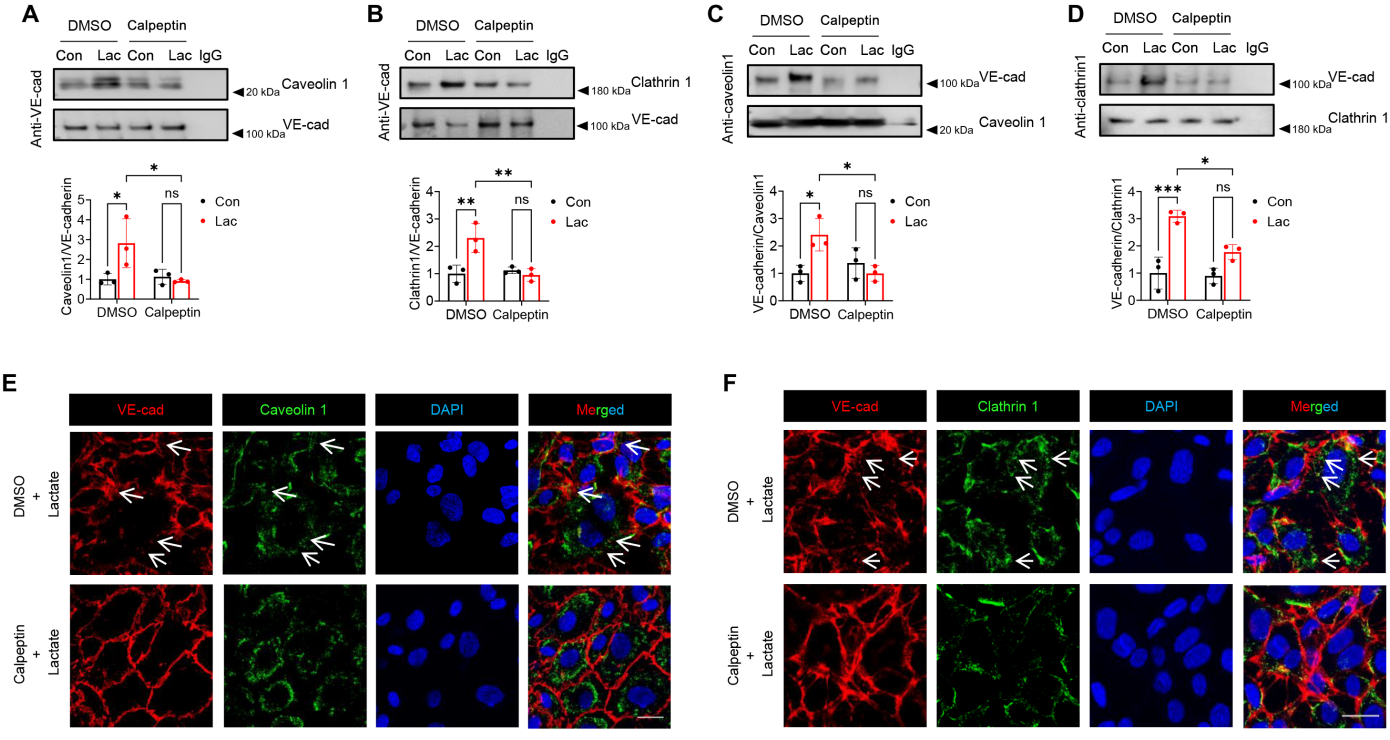

Fig. 6. Calpain activation is required for lactate-induced VE-cadherin endocytosis. (**A** and **B**) HUVECs were treated with calpeptin (10 μM) for 1 hour before lactate stimulation for 6 hours. Protein lysates (200 μg) were precipitated with anti–VE-cadherin antibody followed by immunoblotting with anti-caveolin1 antibody (A) or anti-clathrin1 antibody (B) ($n = 3$). (**C** and **D**) HUVECs were treated with calpeptin (10 μM) for 1 hour before lactate stimulation for 6 hours. Protein lysates (200 μg) were precipitated with anti-caveolin1 antibody (C) or anti-clathrin1 antibody (D) followed by immunoblotting with anti–VE-cadherin antibody ($n = 3$). (**E**) Representative immunofluorescent staining images of VE-cadherin (red), caveolin1 (green), and nuclei (DAPI, blue) in lactate-stimulated HUVECs pretreated with DMSO or calpeptin. White arrows indicate colocalization between VE-cadherin and caveolin1. Scale bar, 20 μm. (**F**) Representative immunofluorescent staining images of VE-cadherin (red), clathrin1 (green), and nuclei (DAPI, blue) in lactate-stimulated HUVECs pretreated with DMSO or calpeptin. White arrows indicate colocalization between VE-cadherin and clathrin1. Scale bar, 20 μm. Two-way ANOVA with Tukey's test (A to D). *$P < 0.05$; **$P < 0.01$; ***$P < 0.001$.

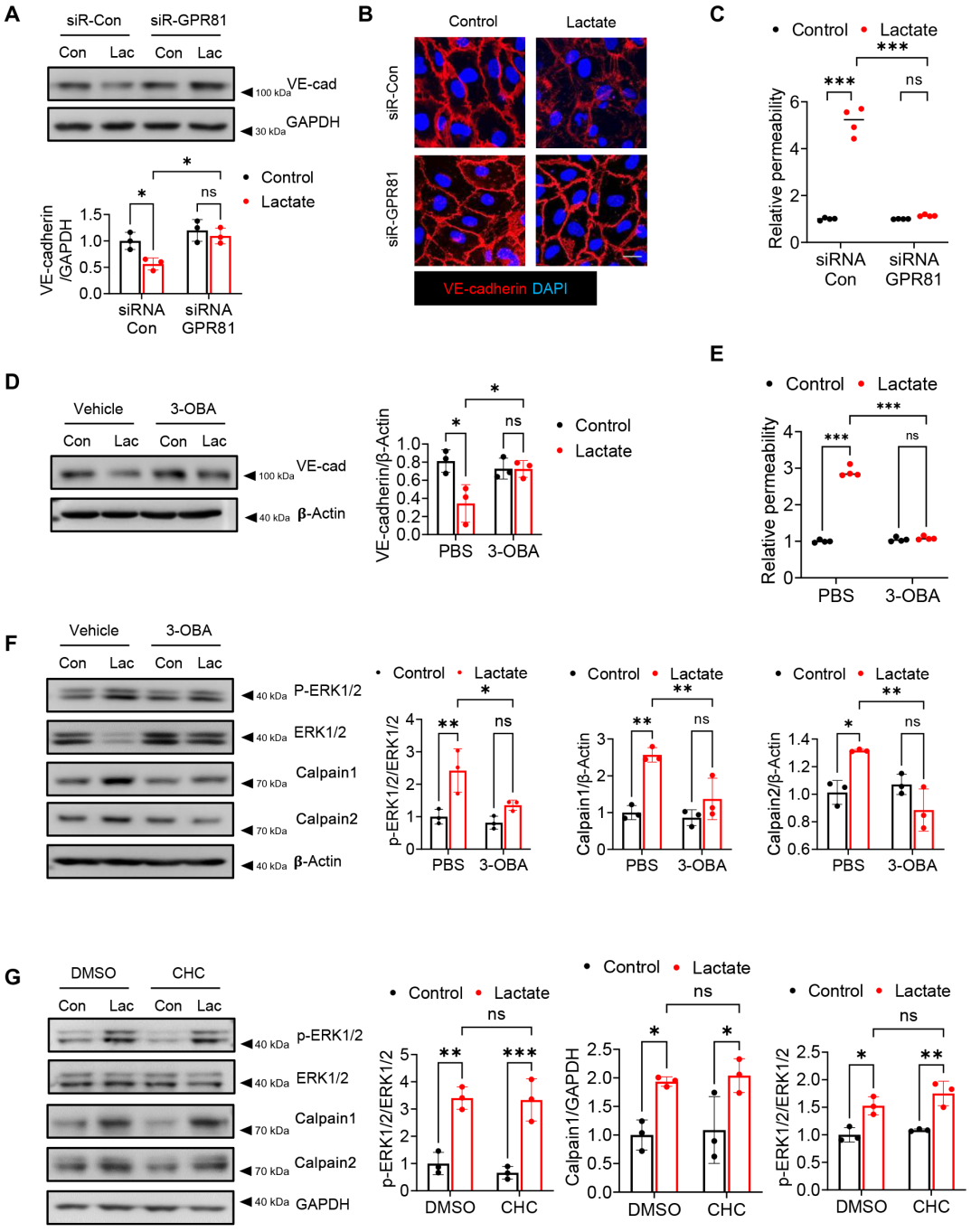

Fig. 7. Lactate-induced VE-cadherin disorganization is mediated by GPR81 signaling. (**A** and **B**) GPR81 was silenced by transfection with specific siRNA for 24 hours before lactate stimulation. Cells transfected with scramble siRNAs were used as controls. VE-cadherin expression was assessed by Western blot (A), and VE-cadherin localization was examined by immunofluorescent staining (B). Scale bar, 20 μm. (**C**) Levels of FITC-dextran penetration through GPR81-silenced HUVEC monolayer upon lactate stimulation ($n = 4$). Cells transfected with scramble siRNAs were used as controls. (**D** and **E**) HUVECs were treated with GPR81 antagonist 3-OBA (5 mM) for 1 hour before lactate stimulation. Expression of VE-cadherin was assessed by Western blot (D) ($n = 3$). Permeability was examined by levels of FITC-dextran penetration through endothelium (E) ($n = 4$). (**F**) HUVECs were treated with GPR81 antagonist 3-OBA (5 mM) for 1 hour before lactate stimulation. Expression of ERK, p-ERK, and calpain1 was assessed by Western blot ($n = 3$). (**G**) HUVECs were treated with an MCT inhibitor (CHC, 3 mM) for 1 hour before lactate stimulation. Expression of ERK, p-ERK, and calpain1 was assessed by Western blot ($n = 3$). Two-way ANOVA with Tukey's test. 3-OBA, 3-hydroxy-butyrate acid. CHC, 2-Cyano-3-(4-hydroxyphenyl)-2-propenoic acid. siR, siRNA. $^*P < 0.05$; $^{**}P < 0.01$; $^{***}P < 0.001$.

of lactate (*18*). To investigate whether MCT1 is involved in lactate-induced activation of ERK1/2 and calpain1/2, we treated ECs with an MCT inhibitor [2-cyano-3-(4-hydroxyphenyl)-2-propenoic acid (CHC)] before lactate stimulation and examined ERK1/2 phosphorylation and calpain1/2 expression. As shown in Fig. 7G, MCT inhibition had no effects on lactate-induced activation of ERK1/2 and calpain1/2.

To validate the critical role of GPR81 signaling, we treated ECs with a specific GPR81 agonist 3,5-Dihydroxybenzoic acid (3,5-DHBA) (*21*) before lactate administration and examined ERK phosphorylation and calpain1/2 levels. We found that GPR81 activation by 3,5-DHBA at 5 mM significantly decreased VE-cadherin levels (fig. S11A) and increased ERK phosphorylation (fig. S11B) and calpain1/2 levels (fig. S11C) in ECs. Collectively, these data suggest that lactate-driven activation of GPR81 signaling contributes to disorganized VE-cadherin, leading to increased endothelium permeability.

Inhibition of GPR81/lactate signaling improves vascular barrier function and prevents death in polymicrobial sepsis

Next, we examined whether in vivo GPR81 inhibition could attenuate sepsis-induced vascular permeability and improve survival outcome. Polymicrobial sepsis was induced by CLP surgery in GPR81 knockout (*GPR81*$^{-/-}$) and WT mice. The expression of GPR81 in heart lysates of WT and *GPR81*$^{-/-}$ mice was examined by Western blot (Fig. 8A). GPR81 deficiency had no effects on sepsis-induced elevation of serum lactate levels (Fig. 8B). Flow cytometry analysis using anti-CD31 and anti–VE-cadherin antibodies showed that sepsis markedly decreased VE-cadherin levels in the ECs of heart (34.9 ± 1.9 versus 43.4 ± 3.1) and liver (6.2 ± 3.4 versus 21.4 ± 2.6) compared with sham controls (Fig. 8C). In contrast, GPR81 deficiency markedly attenuated sepsis-induced decreases in VE-cadherin expressions in the heart and liver tissues (Fig. 8C). Consistently, Western blot analysis showed that knockout of GRP81 protected sepsis-induced decreases in VE-cadherin levels of both heart (Fig. 8D)

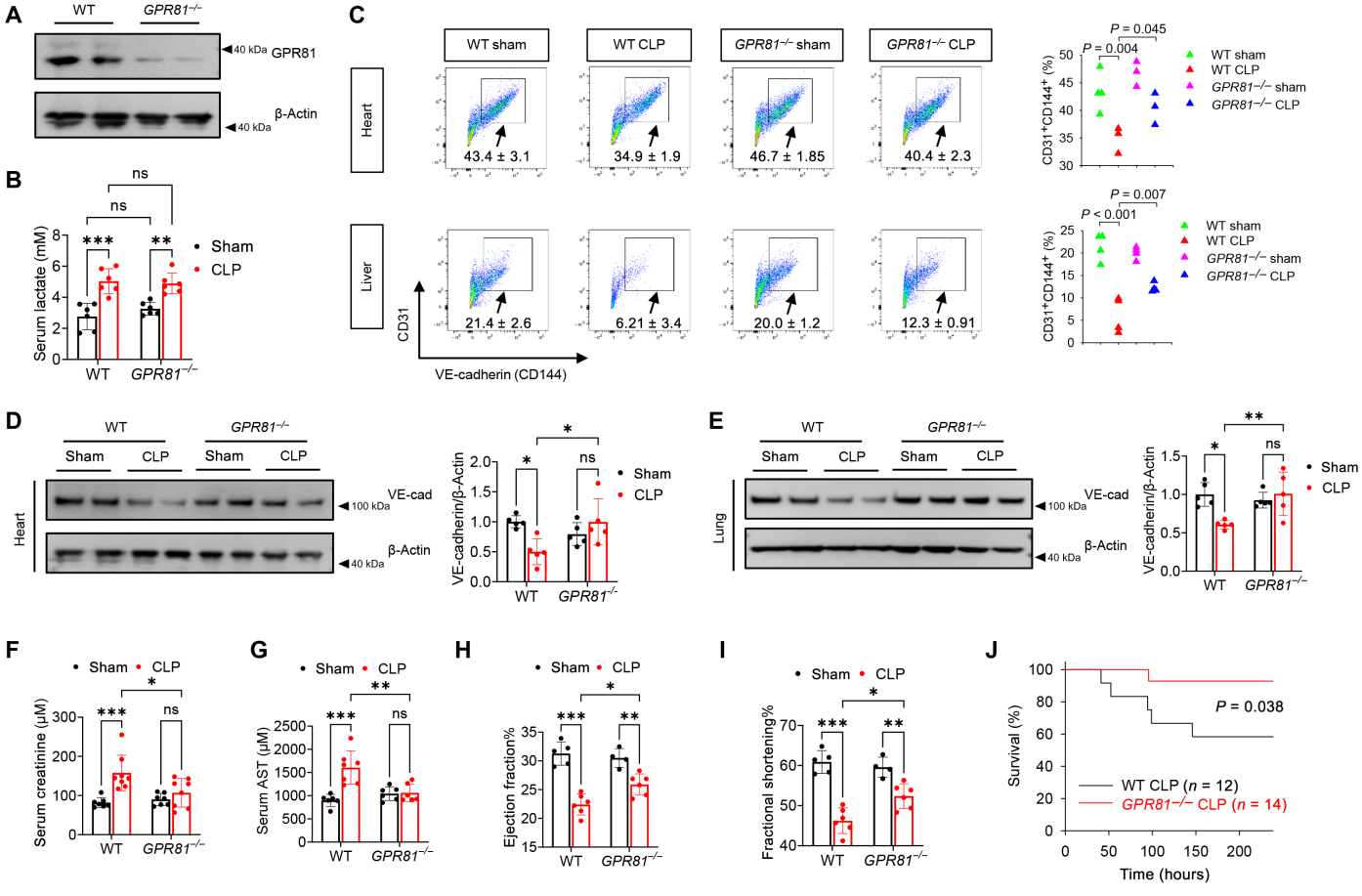

Fig. 8. Inhibition of GPR81 signaling attenuates vascular permeability and improves survival outcomes in polymicrobial sepsis. (**A**) Western blot detection of GPR81 protein expression in whole heart lysates of WT and GPR81 knockout (KO) mice. (**B**) WT and GPR81 KO mice were subjected to CLP or sham surgery. Serum samples were collected 24 hours after surgery, and serum lactate levels were assessed by a commercially available kit ($n = 6$). (**C**) Representative flow density plot and quantitative analysis for VE-cadherin (CD144) positive EC (CD31) frequency in the heart and liver tissues of WT and GPR81 KO mice 24 hours following sham or CLP surgery ($n = 3$ to 4). (**D**) Western blot detection of VE-cadherin protein expression in whole heart lysates of WT and GPR81 KO mice following sham and CLP surgery ($n = 5$). (**E**) Western blot detection of VE-cadherin protein expression in whole lung lysates of WT and GPR81 KO mice following sham and CLP surgery ($n = 5$). (**F** and **G**) Serum levels of creatinine (F) and AST (G) were assessed by commercially available ELISA kits in WT and GPR81 KO mice following sham or CLP surgery ($n = 7$). (**H** and **I**) EF (C) and left ventricular FS (B) were measured 24 hours after CLP/sham surgery in WT and GPR81 KO mice ($n = 4$ to 6). (**J**) Survival outcomes of WT and GPR81 KO mice following sham or CLP surgery were monitored up to 10 days following surgery. Two-way ANOVA with Tukey's test (B to I) and log-rank test (J). *$P < 0.05$; **$P < 0.01$; ***$P < 0.001$.

and lung (Fig. 8E) tissue lysates, when compared to WT septic mice. Next, we examined vascular permeability in WT and *GPR81*$^{-/-}$ mice following CLP/sham surgery. Our data show that GPR81 deficiency significantly attenuated sepsis-induced vascular permeability in the lung (fig. S12A), liver (fig. S12B), and kidney (fig. S12C). In addition, we found that GPR81 deficiency also protected septic mice from lactate supplementation–induced permeability in the lung (fig. S12D), liver (fig. S12E), and kidney (fig. S12F). Moreover, GPR81 deficiency attenuated kidney, liver, and heart dysfunction in septic mice, as evidenced by decreased serum levels of creatinine (Fig. 8I) and AST (Fig. 8J), and increased values of EF (Fig. 8K) and FS (Fig. 8L). Survival outcome analysis showed that GPR81 deficiency improved survival outcome by 59.3% compared with WT septic mice (Fig. 8J). Collectively, our results reveal that GPR81 signaling plays an important role in lactate-induced vascular permeability via promoting VE-cadherin–mediated disruption of adherens junction in ECs.

DISCUSSION

The present study demonstrated a previously unidentified role of lactate, generated from aerobic glycolytic metabolism, in causing vascular barrier dysfunction via disorganizing VE-cadherin in ECs during polymicrobial sepsis. We found that ERK2, not ERK1, interacts with VE-cadherin to stabilize VE-cadherin integrity in resting ECs. However, lactate stimulates its receptor GPR81 to induce ERK1/2 phosphorylation, leading to ERK2 disassociation from VE-cadherin. In addition, lactate-induced ERK1/2 phosphorylation and activation, mediated by GPR81/cAMP/RAF1/MEK signaling, promotes the activation of the cysteine protease calpain1/2 to proteolyze VE-cadherin on the membrane of ECs. The proteolyzed VE-cadherin by calpain1/2 can be internalized by clathrin1- and caveolin1-dependent endocytosis. Suppressed lactate production by glycolysis inhibition or blockage of GPR81/lactate signaling attenuated vascular permeability and multiple organ dysfunction and improved survival outcome of septic mice. A schematic model summarizing these processes is presented in Fig. 9.

In recent years, there has been renewed interest in lactate as a risk marker in the diagnosis of sepsis and septic shock (*11*, *12*). Historically, hyperlactatemia during sepsis was considered as a result of hypoxia (*11*). Recent studies indicate that the origins of sepsis-induced hyperlactatemia are multifactorial, and the lungs are a major source of lactate during sepsis (*11*). Lactate is recycled and cleared from circulation primarily by liver (60%) and kidney (30%) (*47*). We previously reported that polymicrobial sepsis induced multiple organ injuries as early as 6 hours following CLP, which could contribute to elevated serum lactate levels due to reduced lactate clearance (*17*). Clinical evidence shows that the severity of liver disease in septic patients is significantly associated with impaired lactate clearance (*48*). Therefore, to study whether lactate accumulation induces vascular injury, we administrated lactate via intraperitoneal injection 6 hours after CLP-induced sepsis (*17*). We observed that CLP promoted vascular permeability and multiple organ injuries, which was worsened by lactate administration. However, administration of lactate to sham mice had no significant effects on serum lactate levels, vascular permeability, and organ dysfunction. This observation is in agreement with a recent study by Haugen *et al.* (*49*) showing that circulating lactate reaches a peak concentration at 13 min and is back to baseline concentrations after 37 min following lactate injection in sham mice.

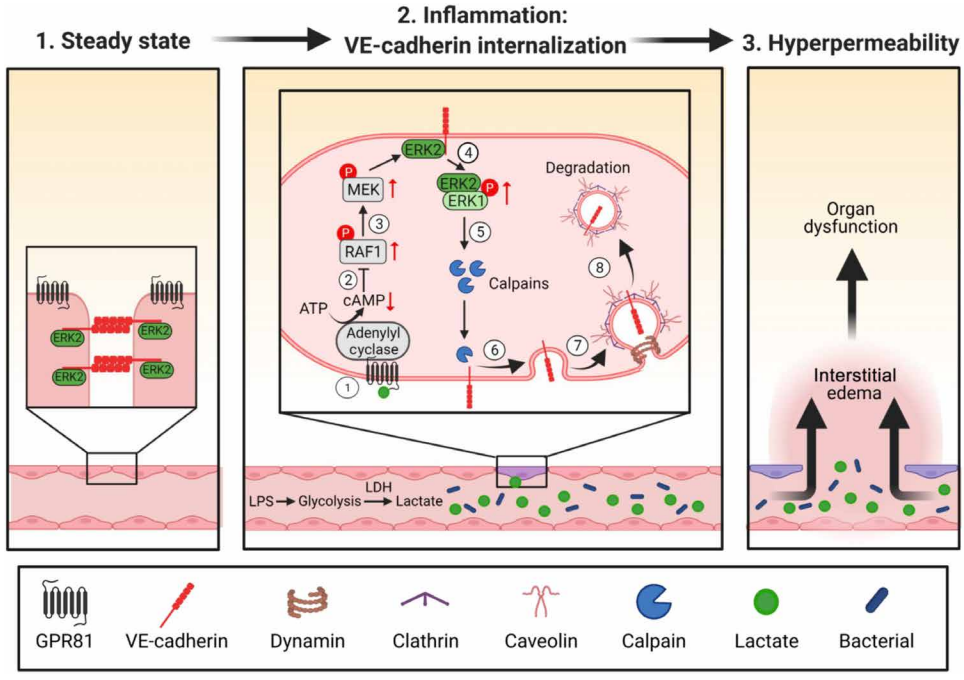

Fig. 9. Scheme of lactate-induced vascular hyperpermeability by promoting VE-cadherin cleavage and endocytosis in sepsis. During sepsis, aerobic glycolysis–derived lactate activates GPR81-dependent signaling in ECs, which results in suppressed cAMP formation and activation of RAF1/MEK/ERK signaling. ERK1/2 phosphorylation induces ERK2 disassociation from VE-cadherin. In addition, lactate induces ERK1/2-dependent activation of calpain1/2 for VE-cadherin cleavage and endocytosis. Endocytosis of VE-cadherin leads to endothelium permeability.

VE-cadherin is the principal cell-cell adhesion molecule of the endothelial adherens junction (*22*). Catenins, such as β-catenin and p120, have been reported to bind with the cytoplasmic domain of VE-cadherin and maintain the endothelial barrier function by stabilizing VE-cadherin at the plasma membrane in ECs (*50*). Our results reveal that ERK2 may also serve as a stabilizer to VE-cadherin complex and maintain VE-cadherin–mediated adherens junction. Previous studies have shown that ERK1/2 signaling plays a critical role in regulating endothelium barrier function (*27*, *51*, *52*). Breslin and colleagues demonstrated that ERK1/2 mediates VEGF signaling cascade leading to endothelial hyperpermeability (*51*). Pharmacological inhibition of MEK/ERK1 signaling abolished VEGF-induced endothelium permeability in vitro (*51*). Consistent with in vitro observations, inhibition of MEK/ERK signaling by trametinib, a Food and Drug Administration–approved MEK1/2 inhibitor, prevented CLP-induced microvascular abnormality and attenuated multiple organ injuries in mice (*53*). In addition, a recent study by Ricard *et al.* (*27*) shows that endothelial-specific deficiency of ERK1/2 leads to hemorrhage in multiple organs, suggesting that ERK1/2 is necessary for endothelium integrity. In this regard, we examined ERK signaling and detected junctional localization of ERK2 in the confluent ECs. Lactate promotes phosphorylation of ERK1 and ERK2 and induces the disassociation between ERKs and VE-cadherin at the plasma membrane, which makes the VE-cadherin more susceptible to proteolytic cleavage. Expression of nonphosphorylatable ERK2 (GFP-ERK2 T183A/Y185F) protected lactate-induced disassociation of ERK2 from VE-cadherin and maintained VE-cadherin integrity in ECs.

Calpain1 (*CAPN1*) and calpain2 (*CAPN2*) are calcium-dependent cysteine proteases that are primarily expressed in ECs (*54*). It has been shown that treatment with septic plasma from endotoxemic mice increased calpain enzyme activity in cultured pulmonary microvascular ECs and caused EC apoptosis (*55*). In addition, EC-specific deletion of calpain showed protective effects on LPS-induced kidney injury (*56*), indicating that calpain activation plays a regulatory role in endothelial injury during inflammation. However, whether calpain could directly disrupt the endothelial barrier by targeting VE-cadherin–mediated adherens junction remains elusive. In the present study, we observed that calpain1 and calpain2 expressions in ECs were increased during CLP-induced sepsis. Administration of supplemental lactate to septic mice further up-regulated calpain1 and calpain2 levels in ECs. Our in vitro studies demonstrated that lactate increased the expression and enzyme activity of calpain1/2, accompanied by VE-cadherin disorganization in ECs. Pharmacological suppression of calpain by its inhibitor or knockdown calpain expression by its specific siRNA prevented lactate-induced VE-cadherin disassembly at the plasma membrane of ECs, suggesting that calpain1/2 activation mediates lactate-induced endothelial barrier dysfunction.

Increased endocytosis and degradation of VE-cadherin is an important mechanism of vascular hyperpermeability during inflammation (*7*, *9*). We also observed that lactate-induced and calpain-mediated proteolytic cleavage of VE-cadherin resulted in VE-cadherin internalization via clathrin1/caveolin1-dependent endocytosis. Either inactivation of calpain1/2 or inhibition of endocytosis with dynamin inhibitor attenuated lactate-induced VE-cadherin endocytosis.

GPR81 is a recently identified receptor for lactate (*18*, *21*, *32*, *46*). We and others have shown that GPR81/lactate signaling plays important roles in regulating immune cell functions during inflammation (*18*, *57*–*59*). A recent study by Khatib-Massalha *et al.* (*21*) showed that activation of GPR81/lactate signaling increases bone marrow endothelium permeability. The mechanism involves suppressed adenylyl cyclase activity and reduced formation of cAMP upon GPR81 activation (*21*, *32*). cAMP directly binds to EPAC, which maintains the VE-cadherin stability through regulating cytoskeleton dynamics (*39*, *40*). In agreement, our data showed that EPAC agonist attenuated lactate-induced VE-cadherin disruption and maintained VE-cadherin proteins in lactate-stimulated ECs. However, EPAC agonist had no effects on lactate-induced ERK1/2 phosphorylation. Notably, cAMP is reported to suppress RAF1/MEK/ERK signaling (*36*, *37*). Enhanced adenylyl cyclase activity by its activator (forskolin), which increased cAMP formation, partially blocked lactate-promoted VE-cadherin disruption and lactate-induced activation of RAF1/MEK/ERK signaling. Our findings, combined with previous findings (*21*, *32*), demonstrated that GPR81/lactate signaling suppresses cAMP formation, resulting in both ERK1/2 activation and EPAC inactivation for VE-cadherin instability. These findings explained the observation that inhibition of MEK/ERK signaling synergizes the permeability-reducing effect of EPAC agonist (*41*). Our data show that pharmacological and genetic inhibition of GPR81 attenuated sepsis-induced vascular permeability and improved survival outcome of septic mice.

Accumulating evidence indicates that lactate is an effector metabolite of aerobic glycolysis that triggers multiple cell signaling and participates in epigenetic regulation of gene transcription (*60*–*62*). Several lines of evidence suggest that lactate alters the function of immune cells during inflammation (*18*, *21*, *57*, *63*, *64*). An important question that should be addressed by future studies is whether lactate could contribute to vascular injury through regulating immune cell functions, such as impaired bacterial clearance and altered cytokine profiles (*65*, *66*). As shown in the current study, elevated serum lactate levels increased blood bacterial burden in CLP-induced polymicrobial sepsis. Therefore, impaired bacterial clearance could also contribute to lactate-induced vascular injury during sepsis. In addition, we have previously reported that lactate promotes high-mobility group box 1 (HMGB1) release from macrophages, leading to endothelium permeability (*18*). However, the mechanism remains unknown. It is reported that HMGB1 transiently induces ERK1/2 phosphorylation in ECs (*67*). Therefore, macrophage-derived HMGB1 could also be a mediator for vascular permeability by activating endothelial ERK1/2 signaling in patients with elevated serum lactate levels.

In summary, the present study demonstrated a previously unknown role of lactate in promoting vascular permeability by inducing VE-cadherin cleavage and endocytosis in ECs. The deleterious effects of lactate in vascular hyperpermeability are mediated by GPR81-dependent signaling, raising the prospect of preventing vascular leakage by selectively interfering with the GPR81/lactate signaling during sepsis.

MATERIALS AND METHODS

Animal information

Tg(Tie2GFP) and WT C57BL/6J mice were purchased from the Jackson Laboratory (Indianapolis, IN). GPR81 knockout ($GPR81^{-/-}$) mice (*32*) were provided by S. Offermanns (Max Planck Institute for Heart and Lung Research, Germany). All mice were maintained and bred at the Division of Laboratory Animal Resources at East Tennessee State University (ETSU). Genotyping of mice was

performed by polymerase chain reaction (PCR) using tail DNA. Age- and sex-matched 8- to 12-week-old mice were randomly included for experiments. Animal experiments were carried out in a blinded fashion.

CLP-induced polymicrobial sepsis model

Mice were randomly allocated into each treatment group. Investigators were blinded to group allocation during data collection and analysis. Polymicrobial sepsis was induced by CLP as described previously (*18*). Briefly, following anesthesia by 5.0% isoflurane, the abdomen was shaved, and the cecum was exposed through a 1-cm midline incision. The cecum was ligated between the third and fourth vascular arcade with a 4-0 silk suture and punctured with a 25-gauge needle. Sham surgically operated mice served as sham controls. Following surgery, a single dose of resuscitative fluid was administrated by subcutaneous injection. Terminal collection of blood was done via the vena cava. Serum was prepared as described elsewhere and stored at −80°C for further experiments.

Endotoxemia model

Endotoxemia was induced in mice by intraperitoneal injection of LPS (10 mg/kg body weight), and the same volume of PBS was injected as controls (*66*).

Bacterial burden assay

Blood samples were collected at 24 hours after CLP and sham surgery and serially diluted with sterile PBS. Sterile dilutions in PBS were inoculated onto both sheep's blood agar and anaerobic blood agar plates. The cultures were incubated 18 to 48 hours under aerobic or anaerobic conditions at 37°C. The anaerobic conditions were achieved by using an anaerobic jar with a GasPak EZ Gas Generating Sachet (Becton Dickinson). The total number of colonies was counted, and colony-forming units per milliliter were calculated.

Enzyme-linked immunosorbent assay

Serum lactate levels were measured by Lactate Assay Kit (Sigma-Aldrich) following the manufacturer's instructions (*18*). Serum levels of creatinine and aspartate aminotransferase (AST) were assessed by commercial kits from Sigma-Aldrich. Tissues were either stored at −80°C or fixed in 4% paraformaldehyde (PFA) for further experiments.

In vivo treatments

To investigate whether increased serum levels of lactate will cause vascular barrier dysfunction, lactic acid (Sigma-Aldrich) was injected intraperitoneally (pH 6.8, 0.5 g/kg body weight) 6 hours following CLP/sham surgery. To suppress lactate production, sodium oxamate (0.75 g/kg body weight) was intraperitoneally injected 3 hours before CLP or sham surgical operation.

In vivo vascular permeability assay

VE barrier function was assessed using the EBD assay, as described previously (*68*). EB (0.5%, dissolved in sterile PBS) was filtered and injected into mice via the penile vein 30 min before mice were sacrificed. Subsequently, mice were perfused with PBS via the left ventricle to remove the intravascular dye. Livers and kidneys were collected, air-dried, and weighted. EBD was extracted in formamide (500 μl) at 55°C for 48 hours. The remaining tissues were pelleted by centrifugation at 2000*g* for 10 min. EBD in tissue supernatants was quantitated by spectrophotometric analysis at 610 nm. Equal volume of formamide was used as blank control.

Echocardiography

Cardiac function was measured by echocardiography 24 hours after induction of CLP sepsis as described previously (*17*). M-mode tracings were used to measure left ventricular wall thickness and left ventricular end-systolic/end-diastolic diameter. Percentage of FS and EF were calculated as previously described (*69*).

Cell culture

HUVECs were purchased from the American Type Culture Collection (ATCC) and cultured in F-12K medium (Kaighn's) supplemented with growth factors (EC growth factor kit-VEGF, ATCC) and 5% fetal bovine serum. HCMECs were purchased from iXCell Biotechnologies and cultured in EC growth medium under conditions suggested by iXCell Biotechnologies. For in vitro lactate treatment, confluent cells were stimulated with 10 mM lactate for 6 hours. In separate experiments, confluent HUVECs were treated with a GPR81 agonist (3,5-DHBA, dissolved in PBS, 2.5 or 5 mM), a GPR81 antagonist (3-OBA, dissolved in PBS, 5 mM), a dynamin inhibitor [Dynasore I (DNSRI), dissolved in dimethyl sulfoxide (DMSO), 20 μM], a calpain inhibitor (calpeptin, dissolved in DMSO, 10 μM), and an ERK inhibitor (LY3214996, dissolved in DMSO, 5 μM) for 1 hour followed by lactate (10 mM) stimulation for 6 hours.

Cell transfection

To silence calpain1, calpain2, MEK1, MEK2, and GPR81, HUVECs (~80% confluence) were transfected with specific siRNAs (40 nmol; Invitrogen) for 24 hours using Lipofectamine 2000. Cells transfected with scramble siRNAs were used as controls. The knockdown efficiency was examined by Western blots with anti-calpain1, anti-calpain2, anti-MEK1/2, and anti-GPR81 antibodies. WT ERK2 (GFP-ERK2) and mutant ERK2 (GFP-ERK2 T183AY185F) plasmids were acquired from Addgene (*31*). WT-ERK2 and MU-ERK2 plasmids were transfected into HUVECs (80% confluence) using Lipofectamine LTX Reagent with PLUS reagent (Thermo Fisher Scientific) for up to 48 hours.

In vitro tube formation assay

Corning Matrigel matrix (stored at −20°C) was thawed at 4°C overnight. Matrigel matrix (100 μl) was added to each well of a 96-well plate followed by incubation at 37°C for 30 min. HUVECs (10^4 cells per well) were seeded on Matrigel-coated wells in medium containing either 10 mM lactate or PBS. Tube formation of HUVECs was photographed 24 hours after incubating at 37°C with 5% CO_2, as described previously (*69*).

Flow cytometry

To detect the cell death and apoptosis, HUVECs treated with lactate or acidified medium (pH 6.0) were stained with annexin V and propidium iodide using the FITC Annexin V Apoptosis Detection Kit (BioLegend) and analyzed by a FACSfortessa flow cytometer (Becton Dickinson). To examine the VE-cadherin expression in primary ECs, tissues were harvested and digested by digestion buffer [collagenase I (1 mg/ml) and collagenase IV (1 mg/ml)] at 37°C. Single-cell suspension was stained with single-color antibodies (outlined in table S1) for 30 min on ice. After washing three times, cells were analyzed using a FACSfortessa

flow cytometer (Becton Dickinson). Results were analyzed by the FlowJo software.

Preparation of cellular membrane and cytosol proteins

Total membrane and cytosol proteins in HUVECs were isolated using the Plasma Membrane Protein Extraction Kit (Abcam) according to the manufacturer's instructions. In brief, cells were lysed using homogenization buffer containing protease inhibitor cocktail. The homogenates were centrifuged for 10 min at 700*g* at 4°C to remove the nucleus. The resulting supernatants were further centrifuged at 10,000*g* for 30 min at 4°C to obtain the total cellular membrane protein. The supernatants were collected as the cytoplasmic fractions. Membrane pellets were dissolved in 0.5% Triton X-100 in PBS. The protein concentrations were determined using a Pierce bicinchoninic acid (BCA) protein assay kit (Thermo Fisher Scientific). The distribution of proteins in the cytosol and membrane fractions were analyzed by Western blot with Na^+/K^+-adenosine triphosphatase (ATP1A1) and glyceraldehyde-3-phosphate dehydrogenase/β-actin as loading controls.

Western blot

Cell lysates were prepared on an ice-cold cell fractionation kit (Abcam) or radioimmunoprecipitation assay buffer containing protease inhibitor (Thermo Fisher Scientific). Lysates were centrifuged at 14,000*g* for 10 min at 4°C. Protein concentration was quantified using the Pierce BCA protein assay kit (Thermo Fisher Scientific). The cellular proteins were separated by SDS–polyacrylamide gel electrophoresis and transferred onto nitrocellulose blotting membranes (GE Healthcare) as described previously (*69*). The membranes were incubated with the appropriate primary antibodies (outlined in the table S1) overnight followed by peroxidase-conjugated secondary antibodies and analysis by the enhanced chemiluminescence system. The signals were quantified using the G:Box gel imaging system by Syngene (Frederick, MD).

Immunoprecipitations

Immunoprecipitations were performed as described elsewhere (*18*). Briefly, 200 μg of total cellular proteins was incubated with antibodies outlined in table S1 overnight at 4°C followed by adding 20 μl of protein A/G-agarose beads (Santa Cruz Biotechnology). The precipitates were washed four times with lysis buffer and boiled in SDS sample buffer. The supernatant was subjected to immunoblotting with appropriate antibodies.

In vitro permeability assay

HUVECs (2×10^5) were cultured on transwell inserts (3.0 μm pore size) of a 24-well plate for 2 days (until confluent). Endothelial monolayer was stimulated with medium containing lactate (10 mM) or acidic medium (pH 6.8) for 6 hours. Then, 100 μl of PBS containing FITC-dextran (1 μg/ml) was added to the upper chamber and 500 μl of PBS was added to the lower chamber. The 24-well plate with transwell inserts was incubated for 5 min, and the concentration of FITC-dextran transferred to the lower chamber was determined using a multimode microplate reader with excitation and emission wavelengths of 492 and 520 nm, respectively.

Calpain activity assay

Calpain activity was assessed using the Calpain Activity Assay Kit (Abcam) according to the manufacturer's protocol. The calpain substrate Ac-Leu-Leu-Tyr-AFC (Ac-LLY-AFC) emits blue light (λ_{max} = 400 nm) and releases free AFC that emits yellow-green fluorescence (λ_{max} = 505 nm) upon cleavage by calpain. AFC release was measured using a microplate spectrophotometer with excitation/emission (Ex/Em) at 400/505 nm.

Immunofluorescence staining

Tissues were collected 24 hours after CLP or sham surgery and fixed in 4% PFA, embedded in paraffin or optimal cutting temperature (O.C.T.) compound, and cut at a 5-mm thickness. Antigen retrieval was achieved by preheating sodium citrate buffer (pH 6.0) for 5 min in a microwave oven, followed by incubation of the slides for 20 min in the boiling citrate buffer. Immunofluorescence staining for cultured cells was performed as described previously (*57*). Briefly, cells were washed with PBS, fixed in 4% PFA, permeabilized with 0.1% Triton X-100, and blocked with 3% bovine serum albumin (BSA) (PBS) at room temperature. Cells were then incubated with primary antibodies diluted in 3% BSA (PBS) overnight at 4°C. After primary antibody incubation at 4°C overnight, signals were developed with Alexa Fluor secondary antibodies (Thermo Fisher Scientific) at room temperature for 30 min. Tissue slides were mounted in Antifade mounting medium with 4′,6-diamidino-2-phenylindole (DAPI) (Vector Laboratories). Images were acquired using a CS SP8 confocal microscope (Leica) and analyzed by ImageJ and ZEN 3.1 software.

Real-time quantitative PCR

HUVECs were treated with lactate or PBS for 2 hours, and total RNA was isolated using RNAzol RT (Molecular Research Center) in accordance with the manufacturer's protocol as previously described (*69*). RNA concentration was measured using Nanodrop 1000 (Thermo Fisher Scientific), and cDNA was synthesized using cDNA reverse kit (Applied Biosystems). Quantitative PCR was performed using specific primers (Applied Biosystems) and TaqMan Universal Master Mix (Applied Biosystems). The mRNA level of CDH5 (forward: 5′-TTGGAACCAGATGCACATTGAT-3′; reverse: 5′-TCTTGCGACTCACGCTTGAC-3′) was normalized to the expression of β-actin.

Statistics

Data were expressed as means ± SD. A Student's *t* test (two-sided) was used to compare two groups affected by one single variable. One-way or two-way analysis of variance (ANOVA) with Tukey's test was used to compare multiple data groups affected by one or two independent variables, respectively. All statistical analyses were carried out using SigmaPlot v11.0 software (Systat Software). Survival differences were determined using the Kaplan-Meier method and the log-rank test. Differences were considered statistically significant at P values of <0.05. The investigators were blinded to the group allocation during the experiment and data collection. On the basis of the power analysis and the extensive experience with the mouse model of CLP sepsis, we estimated the number of mice per group that would be required to detect effects of interest at the $P <$ 0.05 level of significance. The numbers of technical replicates or biological replicates in each group are stated in the figure legends.

Study approval

Animal experiments and euthanasia protocols were performed in accordance with the *Guide for the Care and Use of Laboratory Animals* published by the National Institutes of Health (NIH Publication,

8th Edition, 2011) and approved by the ETSU Committee on Animal Care.

SUPPLEMENTARY MATERIALS

Supplementary material for this article is available at https://science.org/doi/10.1126/sciadv.abm8965

View/request a protocol for this paper from *Bio-protocol*.

REFERENCES AND NOTES

1. M. Singer, C. S. Deutschman, C. W. Seymour, M. Shankar-Hari, D. Annane, M. Bauer, R. Bellomo, G. R. Bernard, J. D. Chiche, C. M. Coopersmith, R. S. Hotchkiss, M. M. Levy, J. C. Marshall, G. S. Martin, S. M. Opal, G. D. Rubenfeld, T. van der Poll, J. L. Vincent, D. C. Angus, The third international consensus definitions for sepsis and septic shock (sepsis-3). *JAMA* **315**, 801–810 (2016).
2. J. Joffre, J. Hellman, C. Ince, H. Ait-Oufella, Endothelial responses in sepsis. *Am. J. Respir. Crit. Care Med.* **202**, 361–370 (2020).
3. N. M. Goldenberg, B. E. Steinberg, A. S. Slutsky, W. L. Lee, Broken barriers: A new take on sepsis pathogenesis. *Sci. Transl. Med.* **3**, 88ps25 (2011).
4. W. Jaffee, S. Hodgins, W. T. McGee, Tissue edema, fluid balance, and patient outcomes in severe sepsis: An organ systems review. *J. Intensive Care Med.* **33**, 502–509 (2018).
5. W. L. Lee, A. S. Slutsky, Sepsis and endothelial permeability. *N. Engl. J. Med.* **363**, 689–691 (2010).
6. R. Chang, J. B. Holcomb, Choice of fluid therapy in the initial management of sepsis, severe sepsis, and septic shock. *Shock* **46**, 17–26 (2016).
7. C. Ince, P. R. Mayeux, T. Nguyen, H. Gomez, J. A. Kellum, G. A. Ospina-Tascon, G. Hernandez, P. Murray, D. De Backer, A. X. Workgroup, The endothelium in sepsis. *Shock* **45**, 259–270 (2016).
8. W. K. Yu, J. B. McNeil, N. E. Wickersham, C. M. Shaver, J. A. Bastarache, L. B. Ware, Vascular endothelial cadherin shedding is more severe in sepsis patients with severe acute kidney injury. *Crit. Care* **23**, 18 (2019).
9. N. R. London, W. Zhu, F. A. Bozza, M. C. Smith, D. M. Greif, L. K. Sorensen, L. Chen, Y. Kaminoh, A. C. Chan, S. F. Passi, C. W. Day, D. L. Barnard, G. A. Zimmerman, M. A. Krasnow, D. Y. Li, Targeting Robo4-dependent Slit signaling to survive the cytokine storm in sepsis and influenza. *Sci. Transl. Med.* **2**, 23ra19 (2010).
10. R. K. Wolfson, E. T. Chiang, J. G. Garcia, HMGB1 induces human lung endothelial cell cytoskeletal rearrangement and barrier disruption. *Microvasc. Res.* **81**, 189–197 (2011).
11. M. Garcia-Alvarez, P. Marik, R. Bellomo, Sepsis-associated hyperlactatemia. *Crit. Care* **18**, 503 (2014).
12. Z. Liu, Z. Meng, Y. Li, J. Zhao, S. Wu, S. Gou, H. Wu, Prognostic accuracy of the serum lactate level, the SOFA score and the qSOFA score for mortality among adults with sepsis. *Scand. J. Trauma Resusc. Emerg. Med.* **27**, 51 (2019).
13. M. Certo, C. H. Tsai, V. Pucino, P. C. Ho, C. Mauro, Lactate modulation of immune responses in inflammatory versus tumour microenvironments. *Nat. Rev. Immunol.* **21**, 151–161 (2021).
14. B. Nolt, F. Tu, X. Wang, T. Ha, R. Winter, D. L. Williams, C. Li, Lactate and immunosuppression in sepsis. *Shock* **49**, 120–125 (2018).
15. D. H. Oh, M. H. Kim, W. Y. Jeong, Y. C. Kim, E. J. Kim, J. E. Song, I. Y. Jung, S. J. Jeong, N. S. Ku, J. Y. Choi, Y. G. Song, J. M. Kim, Risk factors for mortality in patients with low lactate level and septic shock. *J. Microbiol. Immunol. Infect.* **52**, 418–425 (2019).
16. Y. C. Hsu, C. W. Hsu, Septic acute kidney injury patients in emergency department: The risk factors and its correlation to serum lactate. *Am. J. Emerg. Med.* **37**, 204–208 (2019).
17. Z. Zheng, H. Ma, X. Zhang, F. Tu, X. Wang, T. Ha, M. Fan, L. Liu, J. Xu, K. Yu, R. Wang, J. Kalbfleisch, R. Kao, D. Williams, C. Li, Enhanced glycolytic metabolism contributes to cardiac dysfunction in polymicrobial sepsis. *J Infect Dis* **215**, 1396–1406 (2017).
18. K. Yang, M. Fan, X. Wang, J. Xu, Y. Wang, F. Tu, P. S. Gill, T. Ha, L. Liu, D. L. Williams, C. Li, Lactate promotes macrophage HMGB1 lactylation, acetylation, and exosomal release in polymicrobial sepsis. *Cell Death Differ.* **29**, 133–146 (2022).
19. J. Yan, S. Li, S. Li, The role of the liver in sepsis. *Int. Rev. Immunol.* **33**, 498–510 (2014).
20. S. M. Opal, T. van der Poll, Endothelial barrier dysfunction in septic shock. *J. Intern. Med.* **277**, 277–293 (2015).
21. E. Khatib-Massalha, S. Bhattacharya, H. Massalha, A. Biram, K. Golan, O. Kollet, A. Kumari, F. Avemaria, E. Petrovich-Kopitman, S. Gur-Cohen, T. Itkin, I. Brandenburger, A. Spiegel, Z. Shulman, Z. Gerhart-Hines, S. Itzkovitz, M. Gunzer, S. Offermanns, R. Alon, A. Ariel, T. Lapidot, Lactate released by inflammatory bone marrow neutrophils induces their mobilization via endothelial GPR81 signaling. *Nat. Commun.* **11**, 3547 (2020).
22. M. Giannotta, M. Trani, E. Dejana, VE-cadherin and endothelial adherens junctions: Active guardians of vascular integrity. *Dev. Cell* **26**, 441–454 (2013).
23. T. Motoike, S. Loughna, E. Perens, B. L. Roman, W. Liao, T. C. Chau, C. D. Richardson, T. Kawate, J. Kuno, B. M. Weinstein, D. Y. Stainier, T. N. Sato, Universal GFP reporter for the study of vascular development. *Genesis* **28**, 75–81 (2000).
24. S. A. Jesch, T. S. Lewis, N. G. Ahn, A. D. Linstedt, Mitotic phosphorylation of Golgi reassembly stacking protein 55 by mitogen-activated protein kinase ERK2. *Mol. Biol. Cell* **12**, 1811–1817 (2001).
25. E. Wainstein, R. Seger, The dynamic subcellular localization of ERK: Mechanisms of translocation and role in various organelles. *Curr. Opin. Cell Biol.* **39**, 15–20 (2016).
26. D. Iejima, Y. Minegishi, K. Takenaka, A. Siswanto, M. Watanabe, L. Huang, T. Watanabe, F. Tanaka, M. Kuroda, N. Gotoh, FRS2beta, a potential prognostic gene for non-small cell lung cancer, encodes a feedback inhibitor of EGF receptor family members by ERK binding. *Oncogene* **29**, 3087–3099 (2010).
27. N. Ricard, R. P. Scott, C. J. Booth, H. Velazquez, N. A. Cilfone, J. L. Baylon, J. R. Gulcher, S. E. Quaggin, T. W. Chittenden, M. Simons, Endothelial ERK1/2 signaling maintains integrity of the quiescent endothelium. *J. Exp. Med.* **216**, 1874–1890 (2019).
28. R. Lefloch, J. Pouyssegur, P. Lenormand, Single and combined silencing of ERK1 and ERK2 reveals their positive contribution to growth signaling depending on their expression levels. *Mol. Cell. Biol.* **28**, 511–527 (2008).
29. R. Busca, J. Pouyssegur, P. Lenormand, ERK1 and ERK2 Map kinases: Specific roles or functional redundancy? *Front. Cell Dev. Biol.* **4**, 53 (2016).
30. S. F. Krens, M. Corredor-Adamez, S. He, B. E. Snaar-Jagalska, H. P. Spaink, ERK1 and ERK2 MAPK are key regulators of distinct gene sets in zebrafish embryogenesis. *BMC Genomics* **9**, 196 (2008).
31. A. M. Horgan, P. J. Stork, Examining the mechanism of Erk nuclear translocation using green fluorescent protein. *Exp. Cell Res.* **285**, 208–220 (2003).
32. K. Ahmed, S. Tunaru, C. Tang, M. Muller, A. Gille, A. Sassmann, J. Hanson, S. Offermanns, An autocrine lactate loop mediates insulin-dependent inhibition of lipolysis through GPR81. *Cell Metab.* **11**, 311–319 (2010).
33. Z. G. Cui, N. Y. Hong, J. Guan, H. K. Kang, D. H. Lee, Y. K. Lee, D. B. Park, cAMP antagonizes ERK-dependent antiapoptotic action of insulin. *BMB Rep.* **44**, 205–210 (2011).
34. T. Keranen, T. Hommo, E. Moilanen, R. Korhonen, β_2-receptor agonists salbutamol and terbutaline attenuated cytokine production by suppressing ERK pathway through cAMP in macrophages. *Cytokine* **94**, 1–7 (2017).
35. D. Liu, Y. Huang, D. Bu, A. D. Liu, L. Holmberg, Y. Jia, C. Tang, J. Du, H. Jin, Sulfur dioxide inhibits vascular smooth muscle cell proliferation via suppressing the Erk/MAP kinase pathway mediated by cAMP/PKA signaling. *Cell Death Dis.* **5**, e1251 (2014).
36. C. Funaki, R. R. Hodges, D. A. Dartt, Identification of the Raf-1 signaling pathway used by cAMP to inhibit p42/p44 MAPK in rat lacrimal gland acini: Role in potentiation of protein secretion. *Invest. Ophthalmol. Vis. Sci.* **51**, 6321–6328 (2010).
37. C. Ramstad, V. Sundvold, H. K. Johansen, T. Lea, cAMP-dependent protein kinase (PKA) inhibits T cell activation by phosphorylating ser-43 of raf-1 in the MAPK/ERK pathway. *Cell. Signal.* **12**, 557–563 (2000).
38. W. G. Robichaux III, X. Cheng, Intracellular cAMP sensor EPAC: Physiology, pathophysiology, and therapeutics development. *Physiol. Rev.* **98**, 919–1053 (2018).
39. O. L. Roberts, C. Dart, cAMP signalling in the vasculature: The role of Epac (exchange protein directly activated by cAMP). *Biochem. Soc. Trans.* **42**, 89–97 (2014).
40. K. Noda, J. Zhang, S. Fukuhara, S. Kunimoto, M. Yoshimura, N. Mochizuki, Vascular endothelial-cadherin stabilizes at cell-cell junctions by anchoring to circumferential actin bundles through alpha- and beta-catenins in cyclic AMP-Epac-Rap1 signal-activated endothelial cells. *Mol. Biol. Cell* **21**, 584–596 (2010).
41. D. Gunduz, C. Troidl, C. Tanislav, S. Rohrbach, C. Hamm, M. Aslam, Role of PI3K/Akt and MEK/ERK signalling in cAMP/Epac-mediated endothelial barrier stabilisation. *Front. Physiol.* **10**, 1387 (2019).
42. T. Miyazaki, Y. Taketomi, M. Takimoto, X. F. Lei, S. Arita, J. R. Kim-Kaneyama, S. Arata, H. Ohata, H. Ota, M. Murakami, A. Miyazaki, m-Calpain induction in vascular endothelial cells on human and mouse atheromas and its roles in VE-cadherin disorganization and atherosclerosis. *Circulation* **124**, 2522–2532 (2011).
43. H. Chen, S. J. Libertini, Y. Wang, H. J. Kung, P. Ghosh, M. Mudryj, ERK regulates calpain 2-induced androgen receptor proteolysis in CWR22 relapsed prostate tumor cell lines. *J. Biol. Chem.* **285**, 2368–2374 (2010).
44. A. Glading, F. Uberall, S. M. Keyse, D. A. Lauffenburger, A. Wells, Membrane proximal ERK signaling is required for M-calpain activation downstream of epidermal growth factor receptor signaling. *J. Biol. Chem.* **276**, 23341–23348 (2001).
45. G. J. Doherty, H. T. McMahon, Mechanisms of endocytosis. *Annu. Rev. Biochem.* **78**, 857–902 (2009).
46. K. Ahmed, S. Tunaru, S. Offermanns, GPR109A, GPR109B and GPR81, a family of hydroxy-carboxylic acid receptors. *Trends Pharmacol. Sci.* **30**, 557–562 (2009).
47. J. Seheult, G. Fitzpatrick, G. Boran, Lactic acidosis: An update. *Clin. Chem. Lab. Med.* **55**, 322–333 (2017).
48. S. A. Sterling, M. A. Puskarich, A. E. Jones, The effect of liver disease on lactate normalization in severe sepsis and septic shock: A cohort study. *Clin. Exp. Emerg. Med.* **2**, 197–202 (2015).
49. O. P. Haugen, E. M. Vallenari, I. Belhaj, M. C. Smastuen, J. Storm-Mathisen, L. H. Bergersen, I. Amellem, Blood lactate dynamics in awake and anaesthetized mice after intraperitoneal and subcutaneous injections of lactate-sex matters. *PeerJ* **8**, e8328 (2020).

50. D. Schulte, V. Kuppers, N. Dartsch, A. Broermann, H. Li, A. Zarbock, O. Kamenyeva, F. Kiefer, A. Khandoga, S. Massberg, D. Vestweber, Stabilizing the VE-cadherin-catenin complex blocks leukocyte extravasation and vascular permeability. *EMBO J.* **30**, 4157–4170 (2011).
51. J. W. Breslin, P. J. Pappas, J. J. Cerveira, R. W. Hobson II, W. N. Duran, VEGF increases endothelial permeability by separate signaling pathways involving ERK-1/2 and nitric oxide. *Am. J. Physiol. Heart Circ. Physiol.* **284**, H92–H100 (2003).
52. M. H. Wu, S. Y. Yuan, H. J. Granger, The protein kinase MEK1/2 mediate vascular endothelial growth factor- and histamine-induced hyperpermeability in porcine coronary venules. *J. Physiol.* **563**, 95–104 (2005).
53. J. A. Smith, P. R. Mayeux, R. G. Schnellmann, Delayed mitogen-activated protein kinase/extracellular signal-regulated kinase inhibition by trametinib attenuates systemic inflammatory responses and multiple organ injury in murine sepsis. *Crit. Care Med.* **44**, e711–e720 (2016).
54. T. Miyazaki, R. Akasu, A. Miyazaki, Calpain proteolytic systems counteract endothelial cell adaptation to inflammatory environments. *Inflamm. Regen.* **40**, 5 (2020).
55. H. Hu, X. Li, Y. Li, L. Wang, S. Mehta, Q. Feng, R. Chen, T. Peng, Calpain-1 induces apoptosis in pulmonary microvascular endothelial cells under septic conditions. *Microvasc. Res.* **78**, 33–39 (2009).
56. Z. Liu, J. Ji, D. Zheng, L. Su, T. Peng, J. Tang, Protective role of endothelial calpain knockout in lipopolysaccharide-induced acute kidney injury via attenuation of the p38-iNOS pathway and NO/ROS production. *Exp. Mol. Med.* **52**, 702–712 (2020).
57. K. Yang, J. Xu, M. Fan, F. Tu, X. Wang, T. Ha, D. L. Williams, C. Li, Lactate suppresses macrophage pro-inflammatory response to LPS stimulation by inhibition of YAP and NF-κB activation via GPR81-mediated signaling. *Front. Immunol.* **11**, 587913 (2020).
58. J. M. Ratter, H. M. M. Rooijackers, G. J. Hooiveld, A. G. M. Hijmans, B. E. de Galan, C. J. Tack, R. Stienstra, In vitro and in vivo effects of lactate on metabolism and cytokine production of human primary PBMCs and monocytes. *Front. Immunol.* **9**, 2564 (2018).
59. V. Pucino, M. Certo, V. Bulusu, D. Cucchi, K. Goldmann, E. Pontarini, R. Haas, J. Smith, S. E. Headland, K. Blighe, M. Ruscica, F. Humby, M. J. Lewis, J. J. Kamphorst, M. Bombardieri, C. Pitzalis, C. Mauro, Lactate buildup at the site of chronic inflammation promotes disease by inducing $CD4^+$ T cell metabolic rewiring. *Cell Metab.* **30**, 1055–1074.e8 (2019).
60. T. Latham, L. Mackay, D. Sproul, M. Karim, J. Culley, D. J. Harrison, L. Hayward, P. Langridge-Smith, N. Gilbert, B. H. Ramsahoye, Lactate, a product of glycolytic metabolism, inhibits histone deacetylase activity and promotes changes in gene expression. *Nucleic Acids Res.* **40**, 4794–4803 (2012).
61. D. Zhang, Z. Tang, H. Huang, G. Zhou, C. Cui, Y. Weng, W. Liu, S. Kim, S. Lee, M. Perez-Neut, J. Ding, D. Czyz, R. Hu, Z. Ye, M. He, Y. G. Zheng, H. A. Shuman, L. Dai, B. Ren, R. G. Roeder, L. Becker, Y. Zhao, Metabolic regulation of gene expression by histone lactylation. *Nature* **574**, 575–580 (2019).
62. T. D. Bhagat, D. Von Ahrens, M. Dawlaty, Y. Zou, J. Baddour, A. Achreja, H. Zhao, L. Yang, B. Patel, C. Kwak, G. S. Choudhary, S. Gordon-Mitchell, S. Aluri, S. Bhattacharyya, S. Sahu, P. Bhagat, Y. Yu, M. Bartenstein, O. Giricz, M. Suzuki, D. Sohal, S. Gupta, P. A. Guerrero, S. Batra, M. Goggins, U. Steidl, J. Greally, B. Agarwal, K. Pradhan, D. Banerjee, D. Nagrath, A. Maitra, A. Verma, Lactate-mediated epigenetic reprogramming regulates formation of human pancreatic cancer-associated fibroblasts. *eLife* **8**, e50663 (2019).
63. H. L. Caslin, D. Abebayehu, A. Abdul Qayum, T. T. Haque, M. T. Taruselli, P. A. Paez, N. Pondicherry, B. O. Barnstein, L. A. Hoeferlin, C. E. Chalfant, J. J. Ryan, Lactic acid inhibits lipopolysaccharide-induced mast cell function by limiting glycolysis and ATP availability. *J. Immunol.* **203**, 453–464 (2019).
64. M. J. Watson, P. D. A. Vignali, S. J. Mullett, A. E. Overacre-Delgoffe, R. M. Peralta, S. Grebinoski, A. V. Menk, N. L. Rittenhouse, K. DePeaux, R. D. Whetstone, D. A. A. Vignali, T. W. Hand, A. C. Poholek, B. M. Morrison, J. D. Rothstein, S. G. Wendell, G. M. Delgoffe, Metabolic support of tumour-infiltrating regulatory T cells by lactic acid. *Nature* **591**, 645–651 (2021).
65. C. Zhang, The role of inflammatory cytokines in endothelial dysfunction. *Basic Res. Cardiol.* **103**, 398–406 (2008).
66. Y. Li, S. Deng, X. Wang, W. Huang, J. Chen, N. Robbins, X. Mu, K. Essandoh, T. Peng, A. G. Jegga, J. Rubinstein, D. E. Adams, Y. Wang, J. Peng, G. C. Fan, Sectm1a deficiency aggravates inflammation-triggered cardiac dysfunction through disruption of LXRα signalling in macrophages. *Cardiovasc. Res.* **117**, 890–902 (2021).
67. C. Fiuza, M. Bustin, S. Talwar, M. Tropea, E. Gerstenberger, J. H. Shelhamer, A. F. Suffredini, Inflammation-promoting activity of HMGB1 on human microvascular endothelial cells. *Blood* **101**, 2652–2660 (2003).
68. M. Radu, J. Chernoff, An in vivo assay to test blood vessel permeability. *J. Vis. Exp.* e50062 (2013).
69. M. Fan, K. Yang, X. Wang, Y. Wang, F. Tu, T. Ha, L. Liu, D. L. Williams, C. Li, Endothelial cell HSPA12B and yes-associated protein cooperatively regulate angiogenesis following myocardial infarction. *JCI Insight* **5**, –e139640 (2020).

Acknowledgments: We thank S. Offermanns (Max Planck Institute for Heart and Lung Research, Germany) for providing $GPR81^{-/-}$ mice. We thank the Molecular Biological Core Facility (MBCF), the Laser Scanning Confocal Microscope Facility, the Flow Cytometry Core, and the Division of Laboratory Animal Resources (DLAR) at the East Tennessee State University. **Funding:** This work was supported by National Institutes of Health grants HL071837 (C.L.), HL153270 (C.L.), GM083016 (C.L. and D.L.W.), GM119197 (D.L.W.), C06RR0306551 (ETSU), American Heart Association Predoctoral Fellowship 20PRE35120345 (M.F.), and American Heart Association Postdoctoral Fellowship 916710 (M.F.). **Author contributions:** C.L. and K.Y. conceived the study. K.Y., M.F., X.W., J.X., Y.W., P.S.G., T.H., L.L., and J.V.H. designed the research, drafted the manuscript, performed the experiments, and analyzed the data. C.L., D.L.W., and K.Y. directed the study and critically reviewed and revised the manuscript. **Competing interests:** The authors declare that they have no competing interests. **Data and materials availability:** All data needed to evaluate the conclusions in the paper are present in the paper and/or the Supplementary Materials.

Submitted 19 October 2021
Accepted 11 March 2022
Published 27 April 2022
10.1126/sciadv.abm8965